



Degree Project in Vehicle Engineering

Second cycle, 30 credits

Simulation and optimisation of off-road vehicle performances based on user expectations

GIACOMO CORTESE

LEAL NICOLAS

Abstract

This master thesis was performed in collaboration with Öhlins Racing AB, a company that develops advanced suspension technologies for automotive and motorcycle applications, mostly within the motorsport sector. Shock absorbers, which highly influence the vehicle behaviour and thus the global performances of the vehicle, are all the more important for off-road applications. In the past years, Öhlins Racing mostly focused on on-track applications for its automotive sector, but it recently showed its will to be a powerhouse in the off-road sector. The request from Öhlins Racing was to investigate and optimise the performances of off-road vehicle dampers.

This research project started by looking into the modelling of off-road tracks and the modelling of dampers. The next step was to investigate which vehicle performances were relevant for off-roading and which metrics were necessary to evaluate them. Five tests were conducted in order to analyse the following performances: chassis stability, bump absorption, jump, acceleration/braking and steering. For each one of them, the optimised damper parameters were found and their effects on the vehicle's performances were studied. A comparison has then been conducted in order to analyse the acceleration/braking and steering performances of a vehicle optimised for the chassis stability test and for the jump test. The influence of the soft soil was evaluated by conducting a test that involved the vehicle running on rigid soil and on soft soil (dry sand). The influence of the damper's internal friction was also evaluated by conducting tests with and without friction.

The chassis stability test, which consists of driving on an uneven "dune" profile, showed that a soft setup is better for pitch dynamics but much worse for roll dynamics. On the other hand, a setup deemed too stiff induces high damping forces. When facing a bump or a jump, a vehicle equipped with soft damper settings risks, in addition of having a longer settling time, to hit the bump stops. A setting that is too stiff results in high damping forces and high damper velocities and vertical acceleration of the chassis. Low compression damping is used to keep the damping forces low enough. For the jump, a high rebound damping was found necessary to optimise the landing and to avoid a bounce back. Concerning the acceleration and braking behaviour, it was found that the dampers almost exclusively work in the low-speed region and that a soft setup results in many oscillations while a stiff setup slows down the response. The same effect was established for the steering response: a

comparison showed that the chassis stability optimisation is too soft and results in too many oscillations for the acceleration/braking and steering responses, while the jump setting seems to have a behaviour similar to the optimised settings for these tests. The soft soil test showed that the soft soil is acting as if an extra damping was added to the vehicle, with damping forces and velocities being greatly reduced. Finally, it was shown that the internal friction of the damper does not influence its performances, as the friction forces are kept low by Öhlins Racing's technologies.

The study and modelling of the soft soil was quite complicated due to complexity of the field and the lack of concrete studies about its application to vehicle simulations. The soft soil model developed in this thesis is limited and can thus be improved by future works.

Keywords

Dampers, Off-road, Soft soil, Optimisation, Simulations

Sammanfattning

Detta examensarbete utfördes i samarbete med Öhlins Racing AB, ett företag som utvecklar avancerad fjädringsteknik för fordons- och motorcykel-tillämpningar, främst inom motorsportsektorn. Stötdämpare, som i hög grad påverkar fordonets beteende och därmed fordonets globala prestanda, är en viktig komponent speciellt för offroad-tillämpningar. Under de senaste åren har Öhlins Racing mest fokuserat på bantillämpningar för sin fordonssektor, men nyligen visade man sin vilja att bli ett kraftpaket inom offroadsektorn. Önskemålet från Öhlins Racing var att undersöka och optimera prestandan hos dämpare för off-road fordon.

Detta forskningsprojekt började med att undersöka modelleringen av terrängbanor och modelleringen av dämpare. Nästa steg var att undersöka vilka fordonsegenskaper som var relevanta för terrängkörning och vilka mätvärden som var nödvändiga för att utvärdera dem. Fem tester genomfördes för att analysera följande prestanda: chassistabilitet, stötdämpning, hopp, acceleration /bromsning och styrning. För var och en av dem hittades de optimerade dämparparametrarna och deras effekter på fordonets prestanda studerades. En jämförelse har sedan gjorts för att analysera acceleration/bromsning och styrning hos ett fordon som optimerats för chassistabilitetsprovet och för hoppet. Även inverkan av mjuk mark utvärderades genom att utföra ett prov där fordonet kördes på fast mark och på mjuk mark (torr sand). Inverkan av dämparens inre friktion utvärderades också genom att utföra provningar med och utan friktion.

Chassistabilitetstestet, som består av körning på en ojämn sanddynsprofil", visade att en mjuk inställning är bättre för pitchdynamiken men mycket sämre för rollodynamiken. Å andra sidan ger en för styv inställning upphov till höga dämpkrafter. Vid ett gupp eller hopp riskerar ett fordon som är utrustat med mjuka dämparinställningar, förutom att ha en längre insvängningstid, att bottna hårt. En för styv inställning resulterar i höga dämpningskrafter och höga dämparhastigheter samt vertikal acceleration av chassit. Låg kompressionsdämpning används för att hålla dämpningskrafterna tillräckligt låga. För hoppet var en hög rebound-dämpning nödvändig för att optimera landningen och för att undvika en kraftig tillbaka-studs. När det gäller accelerations- och bromsbeteendet visade det sig att dämparna nästan uteslutande arbetar i lågfartsområdet och att en mjuk inställning resulterar i många svängningar medan en styv inställning saktar ner responsen. Samma effekt konstaterades

för styrresponsen: en jämförelse visade att optimeringen av chassistabiliteten är för mjuk och resulterar i för många svängningar för acceleration/bromsning och styrrespons, medan hoppinställningen verkar ha ett beteende som liknar de optimerade inställningarna för dessa tester. Testet med mjuk mark visade att den mjuka marken fungerar som om en extra dämpning hade lagts till fordonet, med dämpningskrafter och hastigheter som reducerades kraftigt. Slutligen visade det sig att dämparens inre friktion inte påverkar dess prestanda, eftersom friktionskrafterna hålls låga av Öhlins Racings teknik.

Studien och modelleringen av den mjuka jorden var ganska komplicerad på grund av områdets komplexitet och bristen på konkreta studier om dess tillämpning på fordonssimuleringar. Den mjukmarksmodell som utvecklats i denna avhandling är begränsad och kan därför förbättras genom framtida arbeten.

Nyckelord

Dämpare, Off-road, Mjuk mark, Optimering, Simuleringar

Preface

This master's thesis is quite particular in that it was conducted by a pair of students. The work was equally divided. The first three weeks, Nicolas was working alone on the project since his home university required a longer project duration; a time that he used to do literature research on dampers and off-roading. Concerning solutions implementation, the theory and methodology was discussed in pair. The work would then be split and achieved individually when it comes to smaller tasks. Analysis and comments were again conducted in pair.

Acknowledgments

First, we would like to express our deepest gratitude to our supervisors at Öhlins Racing, Olov Rosén and Mats Widmark for their support and guidance throughout the thesis. Their valuable help, expressed through expertise, time and effort has been a key factor in the conduction of this research project. Many thanks to Malte Rothhämel, our supervisor at KTH, for his feedback throughout the thesis. We would as well like to thank Anders Bogg, off-road passionate, who had the kindness to take us off-roading at the Botkyrka Motorklubb in southern Stockholm. This was really a fun and valuable experience. Thanks also to Christopher With, from the Swedish Geotechnical Institute, for his insight on soft soil modelling. Finally, thanks to Jonas Jarlmark Näfver who gave us the possibility to conduct this master's thesis at Öhlins Racing.

Stockholm, May 2024

Giacomo Cortese and Nicolas Leal

Contents

| | | |
|----------|--|-----------|
| 1 | Introduction | 1 |
| 1.1 | Background | 1 |
| 1.2 | Problem definition and purpose of the thesis | 1 |
| 1.3 | Limitations | 2 |
| 2 | The damping technology | 3 |
| 2.1 | The damper | 3 |
| 2.1.1 | Role of dampers | 3 |
| 2.1.2 | Types of damping | 4 |
| 2.1.2.1 | Hydraulic damping | 4 |
| 2.1.2.2 | Material damping | 4 |
| 2.1.2.3 | Frictional damping (Coulomb damping) | 5 |
| 2.1.3 | Tuning a damper | 5 |
| 2.2 | Damping technologies at Öhlins Racing | 6 |
| 2.2.1 | Twintube dampers: the example of the TTX | 6 |
| 2.2.2 | Monotube dampers: the example of the STX | 8 |
| 2.2.3 | Other technologies | 9 |
| 2.3 | Modelling of a damper | 10 |
| 2.3.1 | Damper characteristic and chosen parameters | 10 |
| 2.3.1.1 | Linear models | 10 |
| 2.3.1.2 | Industrial damping curves | 10 |
| 2.3.2 | Improvement of the model: specific cases | 11 |
| 2.3.2.1 | Blow-off | 12 |
| 2.3.2.2 | High-speed choke | 12 |
| 2.3.2.3 | Friction | 13 |
| 3 | The off-road environment | 15 |
| 3.1 | Road profile | 15 |
| 3.2 | Soft soil modelling | 16 |

| | | |
|----------|--|-----------|
| 3.2.1 | Soft ground and rigid tyres | 16 |
| 3.2.1.1 | Elastic ground | 16 |
| 3.2.1.2 | Plastic ground | 18 |
| 3.2.2 | Soft ground and soft tyres - Stiffness only | 18 |
| 3.2.3 | Soft ground and soft tyres - Stiffness and damping | 19 |
| 4 | Method and simulations | 21 |
| 4.1 | Simulation environment | 21 |
| 4.1.1 | Batch Simulations | 22 |
| 4.1.2 | Damper model | 22 |
| 4.1.3 | Terrain model | 23 |
| 4.2 | Metrics | 25 |
| 4.3 | Scenarios | 27 |
| 4.3.1 | Chassis stability | 28 |
| 4.3.2 | Bump Absorption | 30 |
| 4.3.3 | Jump | 31 |
| 4.3.4 | Acceleration and braking | 32 |
| 4.3.5 | Steering | 33 |
| 4.3.6 | Acceleration and braking comparison | 34 |
| 4.3.7 | Steering comparison | 34 |
| 4.3.8 | Influence of friction | 35 |
| 4.3.9 | Influence of soft soil | 35 |
| 4.4 | Optimisation process | 35 |
| 4.4.1 | Chassis stability | 36 |
| 4.4.2 | Bump Absorption | 37 |
| 4.4.3 | Jump | 38 |
| 4.4.4 | Acceleration and braking | 38 |
| 4.4.5 | Steering | 38 |
| 5 | Results | 39 |
| 5.1 | Chassis stability | 39 |
| 5.1.1 | Rock Crawling Results | 39 |
| 5.1.2 | Dune riding Results | 42 |
| 5.2 | Bump Absorption | 44 |
| 5.3 | Jump | 48 |
| 5.4 | Acceleration and braking | 51 |
| 5.5 | Steering | 53 |
| 5.5.1 | Step steer | 54 |
| 5.5.2 | Double lane change | 56 |

| | | |
|----------|---|-----------|
| 5.6 | Acceleration and braking test comparison | 57 |
| 5.7 | Steering test comparison | 58 |
| 5.8 | Influence of friction | 60 |
| 5.9 | Influence of soft soil | 60 |
| 6 | Discussions | 62 |
| 6.1 | Chassis stability | 62 |
| 6.2 | Bump Absorption | 63 |
| 6.3 | Jump | 63 |
| 6.4 | Acceleration and braking | 64 |
| 6.5 | Steering | 65 |
| 6.6 | Acceleration and braking comparison | 66 |
| 6.7 | Steering comparison | 66 |
| 6.8 | Influence of friction | 66 |
| 6.9 | Influence of soft soil | 67 |
| 7 | Conclusions and future work | 68 |
| 7.1 | Conclusions | 68 |
| 7.2 | Future work | 69 |
| | References | 70 |
| A | Damping characteristics construction | 73 |
| A.1 | Bilinear curve | 73 |
| A.2 | Quadrilinear curve | 74 |
| A.3 | Blow-off curve | 76 |
| A.4 | High-speed choke curve | 77 |
| B | Chassis stability test results | 78 |
| B.1 | Optimised parameters - chassis stability test | 78 |
| C | Bump absorption test results | 81 |
| C.1 | Optimised parameters - bump absorption test | 81 |
| C.2 | Numerical results - bump absorption test | 82 |
| C.3 | Low-speed bump absorption test (30 km/h) | 83 |
| C.4 | Medium-speed bump absorption test (60 km/h) | 85 |
| C.5 | High-speed bump absorption test (90 km/h) | 88 |

| | | |
|----------|--|-----------|
| D | Jump test results | 90 |
| D.1 | Optimised parameters - jump test | 90 |
| D.2 | Numerical results - jump test | 92 |
| D.3 | Low-speed jump test (30 km/h) | 93 |
| D.4 | Medium-speed jump test (60 km/h) | 94 |
| D.5 | High-speed jump test (90 km/h) | 96 |
| E | Friction results | 98 |

List of Figures

| | | |
|------|--|----|
| 2.1 | Drive fostering low-speed damping - Öhlins Racing testing for Jeep Gladiator suspensions | 6 |
| 2.2 | Drive fostering high-speed damping - off-roading session at Botkyrka Motorklubb | 6 |
| 2.3 | Longitudinal section of a twintube damper [1] | 7 |
| 2.4 | Twintube during compression phase [1] | 7 |
| 2.5 | Twintube during rebound phase [1] | 7 |
| 2.6 | Longitudinal section of a monotube damper [1] | 8 |
| 2.7 | Construction of a damping curve - compression phase | 11 |
| 2.8 | Friction damper block diagram on Simulink. | 14 |
| 3.1 | Recording of road profile during off-road session | 16 |
| 3.2 | Soft ground and rigid tyre - elastic ground | 17 |
| 3.3 | Soft ground and rigid tyre - plastic ground | 18 |
| 3.4 | Double spring model - tyre and soil | 19 |
| 3.5 | Double spring-damper model - tyre and soil | 20 |
| 4.1 | 3D model of the truck used in CarSim | 22 |
| 4.2 | Terrain model made in Simulink | 24 |
| 4.3 | Road profile - low-speed (40 km/h) chassis stability test | 29 |
| 4.4 | Road profile - high-speed (80 km/h) chassis stability test | 30 |
| 4.5 | Road profile - bump absorption test scenario | 30 |
| 4.6 | 3D visualisation of the bump absorption test on CarSim | 31 |
| 4.7 | Road profile - jump test scenario | 32 |
| 4.8 | 3D visualisation of the jump test on CarSim | 32 |
| 4.9 | Speed profile - acceleration and braking test scenario | 33 |
| 4.10 | Damper curves used for the chassis stability analysis | 37 |
| 5.1 | Pitch-roll envelope - low-speed (40 km/h) chassis stability test | 41 |
| 5.2 | Roll rate - low-speed (40 km/h) chassis stability test | 41 |

| | | |
|------|--|----|
| 5.3 | Pitch rate - low-speed (40 km/h) chassis stability test | 42 |
| 5.4 | Pitch-roll envelope - high-speed (80 km/h) chassis stability test | 43 |
| 5.5 | Roll rate - high-speed (80 km/h) chassis stability test | 43 |
| 5.6 | Pitch rate - high-speed (80 km/h) chassis stability test | 44 |
| 5.7 | Damping curves - low-speed (30 km/h) bump absorption test . | 45 |
| 5.8 | Damping curves - medium-speed (60 km/h) bump absorption test | 46 |
| 5.9 | Damping curves - high-speed (90 km/h) bump absorption test . | 46 |
| 5.10 | Damping curves - low-speed (30 km/h) jump test | 48 |
| 5.11 | Damping curves - medium-speed (60 km/h) jump test | 49 |
| 5.12 | Damping curves - high-speed (90 km/h) jump test | 50 |
| 5.13 | Damping curves - acceleration and braking test | 52 |
| 5.14 | Pitch - acceleration and braking test | 53 |
| 5.15 | Pitch rate - acceleration and braking test | 53 |
| 5.16 | Roll - step steer test | 55 |
| 5.17 | Roll rate - step steer test | 55 |
| 5.18 | Load transfer ratio - step steer test | 55 |
| 5.19 | Roll - double lane change test | 56 |
| 5.20 | Roll rate - double lane change test | 56 |
| 5.21 | Load transfer ratio - double lane change test | 57 |
| 5.22 | Pitch comparison - acceleration and braking | 57 |
| 5.23 | Pitch rate comparison - acceleration and braking | 58 |
| 5.24 | Roll comparison - double lane change | 59 |
| 5.25 | Roll rate comparison - double lane change | 59 |
| 5.26 | Load transfer ratio comparison - double lane change | 59 |
| 5.27 | Vertical dynamics - soft soil influence | 60 |
| 5.28 | Pitch-roll envelope - soft soil influence | 61 |
| | | |
| A.1 | Damper characteristics for different values of η - front and rear axle | 73 |
| A.2 | Quadri-linear damper characteristic | 74 |
| A.3 | Quadrilinear damper characteristic - different building method | 75 |
| A.4 | Construction of a damping curve with blow-off - compression phase | 76 |
| A.5 | Construction of a damping curve with high-speed choke - rebound phase | 77 |
| | | |
| B.1 | Damping curves - high-speed (80 km/h) chassis stability test . | 79 |
| B.2 | Damping curves - low-speed (40 km/h) chassis stability test . . | 79 |
| B.3 | Road profile - high-speed (80 km/h) chassis stability test . . . | 80 |

| | | |
|------|--|----|
| B.4 | Road profile - low-speed (40 km/h) chassis stability test | 80 |
| C.1 | Heave - low-speed (30 km/h) bump absorption test | 83 |
| C.2 | Vertical acceleration - low-speed (30 km/h) bump absorption test | 83 |
| C.3 | Pitch - low-speed (30 km/h) bump absorption test | 84 |
| C.4 | Pitch rate - low-speed (30 km/h) bump absorption test | 84 |
| C.5 | Vehicle response - low-speed (30 km/h) bump absorption test | 85 |
| C.6 | Heave - medium-speed (60 km/h) bump absorption test | 85 |
| C.7 | Vertical acceleration - medium-speed (60 km/h) bump absorption test | 86 |
| C.8 | Pitch - medium-speed (60 km/h) bump absorption test | 86 |
| C.9 | Pitch rate - medium-speed (60 km/h) bump absorption test | 87 |
| C.10 | Vehicle response - medium-speed (60 km/h) bump absorption test | 87 |
| C.11 | Heave - high-speed (90 km/h) bump absorption test | 88 |
| C.12 | Vertical acceleration - high-speed (90 km/h) bump absorption test | 88 |
| C.13 | Pitch - high-speed (90 km/h) bump absorption test | 89 |
| C.14 | Pitch rate - high-speed (90 km/h) bump absorption test | 89 |
| C.15 | Vehicle response - high-speed (90 km/h) bump absorption test | 89 |
| D.1 | Pitch - low-speed (30 km/h) jump test | 93 |
| D.2 | Pitch rate - low-speed (30 km/h) jump test | 93 |
| D.3 | Vehicle response - low-speed (30 km/h) jump test | 94 |
| D.4 | Pitch - medium-speed (60 km/h) jump test | 94 |
| D.5 | Pitch rate - medium-speed (60 km/h) jump test | 95 |
| D.6 | Vehicle response - medium-speed (60 km/h) jump test | 95 |
| D.7 | Pitch - high-speed (90 km/h) jump test | 96 |
| D.8 | Pitch rate - high-speed (90 km/h) jump test | 96 |
| D.9 | Vehicle response - high-speed (90 km/h) jump test | 97 |

List of Tables

| | | |
|-----|---|----|
| 4.1 | Vehicle Specifications | 22 |
| 5.1 | Numerical results - low-speed (40 km/h) chassis stability test . | 40 |
| 5.2 | Numerical results - high-speed (80 km/h) chassis stability test . | 42 |
| 5.3 | Optimised parameters - acceleration and braking test | 52 |
| 5.4 | Optimised parameters - steering tests | 54 |
| 5.5 | Bleed coefficients for comparison tests | 57 |
| 5.6 | Numerical results - soft soil influence | 61 |
| B.1 | Optimised parameters - chassis stability | 78 |
| C.1 | Optimised parameters - bump absorption test | 81 |
| C.2 | Numerical results - bump absorption test | 82 |
| D.1 | Optimised parameters - jump test | 91 |
| D.2 | Numerical results - jump test | 92 |
| E.1 | Numerical results - friction comparison | 98 |

Chapter 1

Introduction

This master thesis project has been carried out in cooperation with Öhlins Racing AB. Located in Upplands Väsby (Sweden), the company develops advanced suspension technologies for automotive and motorcycle applications, mostly within the motorsport sector. Founded in 1976 by Kenth Öhlin, who started to focus on the development of shock absorbers for racing motocross, Öhlins Racing is now present on all the branches of the motorsport market.

1.1 Background

No matter the intended application of the vehicle, ride comfort and handling performance are always in the equation when evaluating vehicle dynamic performances. Shock absorbers highly influence the vehicle behaviour and thus the its global performances. That affirmation is all the more true for off-roading. Off-roading is the fact of driving a vehicle away from public roads, usually on rough terrains such as unpaved roads, sand, mud, snow, rocks etc.

1.2 Problem definition and purpose of the thesis

The goal of this project is to analyse and optimise the performance of off-road shock absorbers. This can be evaluated by several specific scenarios characterised by particular metrics, and is dictated by several parameters. The tuning of those parameters implies a high variation of performance. The

present work aims to study the effect of the parameters tuning on the vehicle performances, with a view to optimise ride handling and vehicle motions through simulations.

This thesis should tackle and answer the following questions:

- What types of road profile are relevant for the evaluation of off-road performances?
- How to model and implement in the simulation environment the interaction between the soft soil and the tyres?
- How should the damper be modelled and which parameters should be adjustable in the damper model?
- Which performances should be evaluated?
- Which tests should be conducted?
- How do the adjustments of the damper parameters affect the performance metrics in the different scenarios under consideration?

1.3 Limitations

Some limitations have been made during this project, for both time and scope reasons.

- The development of the soft soil model was limited due to time restrictions. The limitation of the model is explained in detail in Section 3.2.
- The internal dynamic behaviour of the damper has not been modelled. It is considered to be the same for every damper, regardless of its damper curve.

Chapter 2

The damping technology

The damper has always been a key component in a vehicle, all the more for off-road vehicles. In this chapter, the general knowledge about them is studied, as well as the damping technologies developed at Öhlins Racing and the modelling of dampers.

2.1 The damper

In this section, the role of dampers and the different types used in the industry are tackled. Their tuning is also studied.

2.1.1 Role of dampers

The principle behind the functioning of a damper is pretty simple. Still, the technology is reliable and necessary for a good vehicle ride.

Dampers are coupled with springs. Springs exert force based on how much they are compressed (which might not follow a linear pattern), while dampers produce force based on the velocity of the compression. Springs support the vehicle's static weight, while dampers control its dynamic movements. The study of the springs is not a matter of importance in this thesis, but one can still know that many different technologies exist, the most widely used being the ones made out of steel or fibre composites (leaf, torsion and coil springs). Elastomer, air and gas-hydraulic springs are also used on a smaller scale and for specific applications. Öhlins Racing uses coil springs for most automotive applications, as their low maintenance, weight and cost as well as their compactness and their ease of coupling with dampers make them a

reliable technology to accompany shock absorbers. They are preloaded and operate in compression.

A shock absorber is composed of a body, a shaft and a piston. When the vehicle faces a change in the road profile, a bump or a pothole for example, the piston will move up or down, creating a movement of the fluid through the valves in the piston or in the base of the tube (see monotube and twintube section for a detailed explanation) resulting in a damping force. Note that even though it is not the case in reality, the fluid is considered non-compressible in this study. It needs room to move to when absorbing a shock. This room needs to be created by the compression of a gas. Whether there is the presence of a separating piston or not (otherwise the damper is an emulsion damper), the gas used is usually nitrogen as it is an inert gas avert to react chemically with the rubber seals and greases used. Its temperature is also very stable [1].

2.1.2 Types of damping

2.1.2.1 Hydraulic damping

Hydraulic damping is the most common type of damping and is widely used in automotive for shock absorbers. The source of damping is the energy losses occurring when the piston moves against the fluid in the damping system (cylinder filled with liquid). The damping force is a function of the velocity, volume and shape of the piston. In comparison to the other types of damping discussed in this section, hydraulic damping is more effective in terms of dynamics since it is dependant of the velocity, it isolates high frequencies and it is easily adjustable. This type of damping will be discussed later in this thesis as it is the type of damping used by Öhlins Racing for their shock absorbers systems.

2.1.2.2 Material damping

Material damping is due to molecular interactions happening inside of a material. During the oscillation, internal friction is created, which results in a dissipation of energy (usually as heat losses) and thus a reduction of oscillation movement. When the material suffers the deformation, it loses energy according to a hysteresis cycle with the force being dependant of the extension of the system and not of the excitation frequency. This type of damping is used for metallic materials and is inadequate for vehicle suspensions. It is usually used in household electrical, with isolator pads put under devices

subject to high levels of vibration (washing-machines, refrigerator etc.) in order to dissipate the energy and prevent it to spread into the floor [2]. It is used in rubber suspensions of lightweight trailers in the automotive sector.

2.1.2.3 Frictional damping (Coulomb damping)

Another type of damping is frictional damping. Also called Coulomb damping (due to the forces involved), it rests on the energy losses due to frictions between the parts of the systems. In addition to heat, it also generates noise, wear, and non-linear dynamic effects such as stick slip. Those effects are very unwanted in a vehicle, thus the rare use of this damping in the automotive industry (they are only used in cheap applications of steering dampers, for instance in motorcycles with sidecars). As a matter of fact, it is used in the building industry, some seismic dampers using the Coulomb damping principle [2].

2.1.3 Tuning a damper

The damping of a shock is composed of two phases:

- **Compression:** when the vehicle hits a bump, the piston makes a vertical upward movement and advances into the oil of the shock absorber. The damper compresses and dissipates energy.
- **Rebound:** after the bump, the energy stored by the springs is released. The piston moves downward to increase the length of the shock absorber and create contact again between the wheel and the ground.

The internal movement of the oil flow is explained later for monotube and twintube technologies.

For optimal performance, the desired amount of damping is depending on damper velocity and travel direction. Depending on the model, Öhlins' shock absorbers may be adjustable in low- and high-speed region individually, for both compression and rebound motion. Note that high-speed or low-speed refer to the velocity of the piston, not to the velocity of the vehicle.

Low-speed damping occurs on relatively flat roads and for a quite steady steering input, for instance high speed driving in the desert or on thin snow, as shown in Figure 2.1. The compression should not be too fast, but one still need to have it fast enough to respond to small bumps. However, adjustments



Figure 2.1: Drive fostering low-speed damping - Öhlins Racing testing for Jeep Gladiator suspensions



Figure 2.2: Drive fostering high-speed damping - off-roading session at Botkyrka Motorklubb

for low-speed rebound are more complicated than for compression. The tyres need to keep contact with the ground as much as possible without the ride being too bouncy.

For high-speed damping, the damping is increased as well as the stiffness of the ride. The tuning is very different than for the low-speed damping. High-speed damping usually occurs on very uneven road profiles with quite slow but shaky manoeuvres, such as 4x4 trial (see Figure 2.2), or for heavy impacts such as jump landings.

2.2 Damping technologies at Öhlins Racing

As written before, land vehicle suspensions manufacturers and thus Öhlins Racing use hydraulic damping. There are two types of hydraulic dampers used by Öhlins Racing: twintube and monotube.

2.2.1 Twintube dampers: the example of the TTX

In twintubes, tubes are co-axial and one is inside of the other. The inner tube is called the pressure tube and inside of it is the piston. The piston has both compression and rebound valves splitting the pressure chamber in two. At the bottom, base valves control the flow of oil between the side chamber and the lower pressure chamber (see Figure 2.3). During the compression phase, the piston is pushed down. Some of the oil in the lower pressure chamber will pass through the piston (compression valves are opened) and go to the upper pressure chamber. A volume of the oil in the lower pressure chamber, equal to

the rod volume, will pass through the base valves to go to the side chamber, as seen in Figure 2.4. During the rebound phase, the oil flows will go the opposite way since the rebound valves open, and the length of the damper will extend, as shown by Figure 2.5.[1]

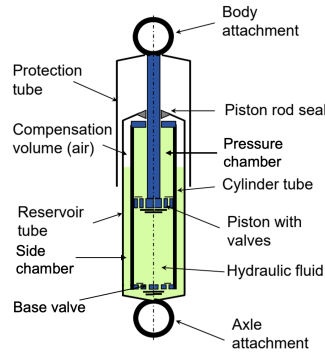


Figure 2.3: Longitudinal section of a twintube damper [1]

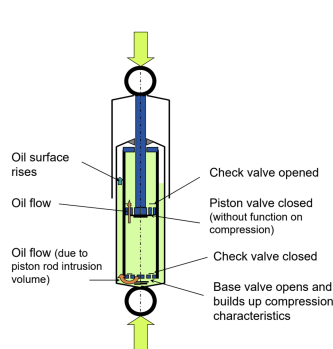


Figure 2.4: Twintube during compression phase [1]

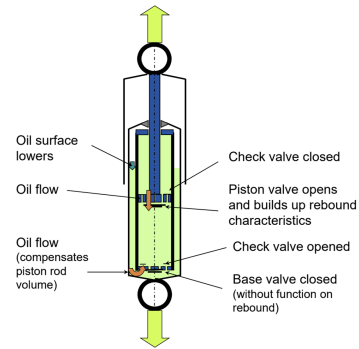


Figure 2.5: Twintube during rebound phase [1]

An example of a twintube damper developed by Öhlins is the TTX technology. First introduced in 1996, this damper technology is responsible for the win of more than 100 World Championships.

Three different types of valves are commonly used: bleed, shim and poppet valves. The bleed and poppet valves are in parallel for both compression and rebound. The bleed valves are the low-speed compression valves. The poppet valves, which are the high-speed valves, are preloaded by coil springs by an external adjustment. These are compact and precise. On top of a poppet valve

can be placed shim stacks; the valve is then called a shim valve. Shim stacks are used to modify the opening characteristics of the poppet valves. [3]

2.2.2 Monotube dampers: the example of the STX

There is only one tube and one oil chamber in a monotube damper. The valves are located in the piston. A separator divides the oil chamber and the gas chamber, as it can be seen in Figure 2.6. During the compression phase, the piston is pushed down. Some of the oil flows to the upper part of the oil chamber, passing through the compression valves. Some of the oil in the lower part will be pushed down. Since there are no base valves leading to a side chamber, the oil cannot flow to the non-existent side chamber, and thus pushes on the separator downward. However, since the gas in the gas chamber is compressible, the downward movement of the separator is allowed. A pressure drop is created. During the rebound phase, it happens the opposite way, extending the length of the damper. [1]

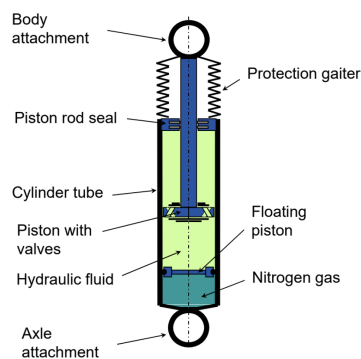


Figure 2.6: Longitudinal section of a monotube damper [1]

The monotube has some advantages over the twintube. It has better cooling properties and a better response rate. The piston can be larger for the same outer dimensions. However, such system is more complicated to install and evidently more costly since it requires high precision components. Moreover, the TTX twintube is almost cavitation free while there is a high risk of cavitation in monotube dampers.

An example of a monotube damping technology developed by Öhlins Racing is the STX technology. It is widely used in off-road applications. It

rests on the monotube design, with the gas chamber usually being situated in another compartment, either externally connected by a hose or directly mounted on the shock absorber. Öhlins Racing uses nitrogen gas N_2 as a compressible gas. The presence of compressible gas prevents the phenomenon of cavitation in the shock absorber. Cavitation results in the creation and implosion of air bubbles in the fluid, entailing a certain number of unwanted effects, such as vibrations and heat generation, responsible for a lower service life of the shock absorber, and more importantly the impossibility to generate a sufficient damping force.

2.2.3 Other technologies

Some technologies exist in order to improve the damping.

In a position sensitive damping (PSD) damper, a set-up used on twintubes, the central part of the inner tube is equipped with grooves, which allow the oil to flow around the piston, resulting in a smaller pressure loss in this zone (comfort zone) in comparison to the others (control zones). The damping can be controlled according to the number of grooves and their length [4].

Another technology is the acceleration sensitive damping (ASD), used in both monotube and twintube. It controls the damping speed over the piston according to the number of valves opened. In order for the piston to move faster, a spring-controlled ASD valve opens when the acceleration of the piston is high enough. There is then more space for the oil to flow and a quicker movement of the piston. When the car passes a bump slowly, the piston doesn't accelerate fast enough so the compression remains resistant entailing a high stiffness. When the piston accelerates faster, the compression remains less resistant and the piston movement is faster, assuring a soft damping and smooth ride.

Another interesting set-up is the magnetorheological technology. The fluid used is magnetorheological and is filled with iron particles. It reacts with a magnet placed in the piston in order to change the viscosity of the fluid by rearranging its particles, resulting in an increase or a decrease of the piston movement.

2.3 Modelling of a damper

In this section, it will be explained how the dampers theoretical model was built. It will explain the journey from the simplest damping model to the most complex one that was developed.

2.3.1 Damper characteristic and chosen parameters

2.3.1.1 Linear models

When the model is reduced to the simplest complexity, a shock absorber can be described by only one parameter : the damping coefficient. It is the ratio between the damping force and the shaft velocity. The higher the damping coefficient, the higher the shock absorption. It defines the shape of the damping characteristic $F = f(v)$ with F the damping force and v the velocity of the damper, also known as damper velocity.

A damping curve is composed of two phases: the compression and the rebound curves. The compression is characterised by positive damping velocities and damping forces while those values are negative for the rebound phase.

The simplest model of a shock absorbing system is a damper with a damping coefficient c . The damping force is $F = c \cdot v$ with v the velocity of the damping, for both the compression and the rebound phase. The curve is linear, and the slope is characterised by the damping coefficient.

For some initial studies on damper behaviour the linear model was also expanded as a continuous piecewise function where every segment was defined by a straight line. This started as a bilinear model where the inclination for compression and rebound was different and was further expanded in a quadrilinear model to define a low and high speed region for both strokes. The curves for these models can be found in appendix A.1 and A.2.

2.3.1.2 Industrial damping curves

The dampers used in the industry are actually more complex than the models explained previously. The damping curves of such dampers rest on the settings of its valves. In the damper, the bleed and the high-speed valves

(HSV) are in parallel.

The bleed valve has a quadratic force that can be written $F_{\text{bleed}} = K_{\text{bleed}} \cdot v^2$ with F_{bleed} the damping curve of the bleed, K_{bleed} the bleed coefficient and v the damping velocity. This equation comes from the behaviour of flow through small orifices [5], with K_{bleed} being dependant of many parameters. It can still be understood how higher bleed coefficient correspond to higher damping values and, physically, smaller orifices.

The high-speed valve has a curve composed of an affine and an exponential part. It can be a poppet valve or a shim valve. It is equal to:

$$F_{\text{HSV}} = (1 - e^{-\alpha v})(\beta_{\text{HSV}} + \delta_{\text{HSV}} \cdot v)$$

With F_{HSV} the damping force of the poppet valve, α the exponential parameter (fixed to a value of 100), β_{HSV} the offset, δ_{HSV} the slope and v the damping velocity. Combined in a parallel configuration, the bleed and the poppet valve end up giving the curve represented in Figure 2.7.

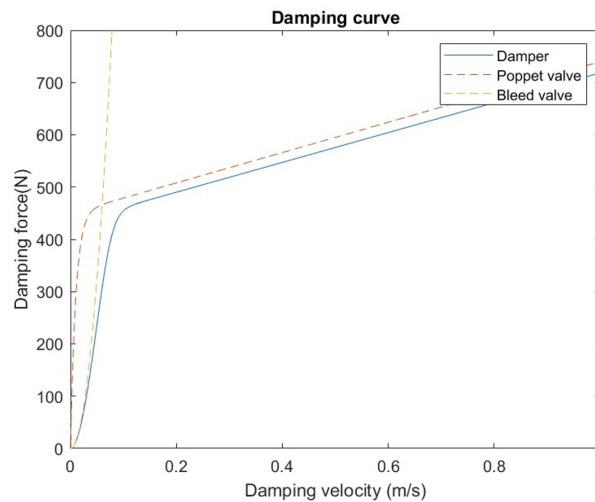


Figure 2.7: Construction of a damping curve - compression phase

2.3.2 Improvement of the model: specific cases

The first section of this chapter tackled the parameters characterising a shock absorber as well as the damping curves resulting from the configuration

and combination of those parameters. However, the previous damping curves displayed are the simplest versions and are used to describe shock absorbers in the most usual conditions. Some peculiar uses or road configurations require particular parameters and characteristics. This section discusses some specific cases.

2.3.2.1 Blow-off

When subject to high impacts, such as jump landings, the damping force can become too high and transfer too much force to the attachment points and the damper itself. This can lead to some critical scenarios and safety issues such as the failure of components. However, providing enough force to ensure proper deceleration and to avoid hitting the bump stops with too much force is also critical. This balance was best described during internal discussions as: “sometimes one needs to choose between breaking the dampers or breaking the car”. For high damping velocities, it can be reasonable to prevent the damping force from being too high and to make the force constant after a certain threshold. This characteristic, added on the compression curve, is named blow-off. It is achieved by putting a blow-off valve in parallel to the bleed valve and the high-speed valve. If the pressure inside the chamber is too high, the blow-off valve opens and stops the increase of the damping force [6]. The parameter to control is the preload force, which dictates at what point the blow-off valve opens. The equation of the blow-off curve is:

$$F_{\text{blow-off}} = \beta_{\text{blow-off}} + K_{\text{blow-off}} \cdot v^2$$

With $F_{\text{blow-off}}$ the damping force of the blow-off valve, $\beta_{\text{blow-off}}$ the blow-off offset, $K_{\text{blow-off}}$ the blow-off coefficient and v the damping velocity. The curve is represented in Figure A.4.

2.3.2.2 High-speed choke

Unlike the compression blow-off discussed previously, it can be interesting to increase the damping force after a certain level for the compression or the rebound phase. This high-speed choke configuration, which highly increases the damping force when the velocity becomes important, can for instance prevent bottoming out when jumping. An additional valve is put in series with the high-speed valve, by restricting the lift height of the latter. The parameters that need to be controlled are the bleed coefficient and the preload on the valve.

In this study, the high-speed choke has been implemented for the rebound phase only. The equation of the high-speed choke curve is:

$$F_{\text{HSC}} = K_{\text{HSC}} \cdot v^2$$

With F_{HSC} the damping force of the high-speed choke, K_{HSC} the high-speed choke coefficient and v the damping velocity. The curve is represented in Figure A.5.

2.3.2.3 Friction

A shock absorber is a mechanical system whose internal components interact with each other. Thus, friction naturally occurs between the moving part (the piston and the chamber cylinder).

The friction is defined by a dynamic friction F_d and a static friction F_s . Those values have been chosen as $F_d = 16N$ and $F_s = 23N$ after careful reading of the Öhlins TTX's information book [3].

A common friction model rests on two conditions, one on the damping force and the other on the damping velocity. When the damping force is lower than the static friction, the friction force is equal to the damping force. When the damping force becomes higher than the static friction, the friction force is equal to the static friction. It remains so until the damper velocity passes a certain velocity threshold and leaves the following interval $[-v_{\text{threshold}} ; v_{\text{threshold}}]$. The friction force is then equal to the dynamic friction. This friction is the Coulomb friction model [7]. This is modelled in the Simulink block diagram displayed in Figure 2.8.

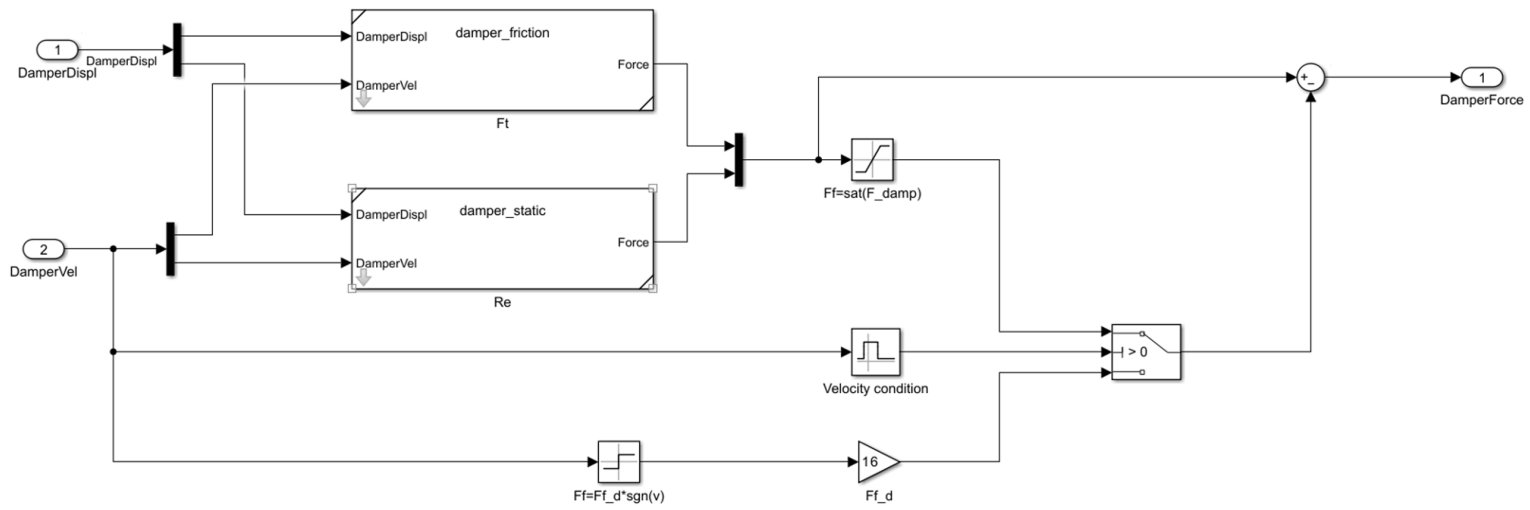


Figure 2.8: Friction damper block diagram on Simulink.

Chapter 3

The off-road environment

Off-roading is different from any other kind of racing, not only in vehicles and racing format but especially in terrain. The off-road environment is very peculiar, both in terms of road profile and also on the driving surface. Off-road profiles and soft soil modelling are dealt with in this chapter.

3.1 Road profile

One of the characteristics of off-roading is the peculiar aspect of the road. An off-road track is very different from other classical racing tracks. It is made of bumps, jumps, ditches, hills, etc. Those segments can occur randomly in the track since it is subject to the natural aspect of the road (desert, forest, etc.) and it is thus very hard to define a typical road profile.

A lot of research has been conducted but very few information relevant for the thesis was found. Indeed, entities detaining such data are usually car manufacturers and OEMs, which spend a lot of money acquiring such information, and were not keen on sharing it for the purpose of this thesis. Some data was thus acquired empirically during an off-roading session in a car equipped with accelerometers. This data, shown in Figure 3.1, was used as a baseline to construct the final road profiles. After some analysis and tuning, the rough-road profile was modelled as a band-pass filtered white noise.



Figure 3.1: Recording of road profile during off-road session

3.2 Soft soil modelling

Apart from the road profile, off-road tracks are different from classic tracks for one main reason: the characteristics of the ground. Off-roading can be referred to as driving on every terrain that is not asphalt. It can be everything such as: sand, snow, mud, gravel etc. All are different from asphalt and from each other. This results in different interactions between the car and the ground. Modelling the soil is thus of primary importance in the simulations since results can drastically vary according to how the ground was modelled. Different approaches of soft soil modelling have been studied and will be presented. The model chosen will be explained at the end of this section.

3.2.1 Soft ground and rigid tyres

3.2.1.1 Elastic ground

The first approach studied is to consider only the elasticity of the ground, while the tyre is considered fully rigid. This can be a good approximation when the soil stiffness is much lower than the tyre's. This is not always a good approximation since tyres are usually purposefully deflated (and therefore less stiff) during off-road applications, but this assumption will be relaxed later. In this scenario, when the tyre is rolling on soft soil, it sinks. The distance between the nominal height of the road and the lowest point of the tyre is

called sinkage. This is represented by the variable z_0 in Figure 3.2, the wheel drawn in blue and the road in black.

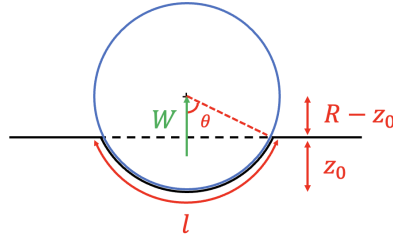


Figure 3.2: Soft ground and rigid tyre - elastic ground

In this case, it is considered that the ground is deformed only while in contact with the tyres and then it goes back to its initial state after the passage of the tyres. This is a perfectly elastic behaviour. The Bekker pressure-sinkage relation [8] defines the normal pressure on the tyre depending on the sinkage. The equation is :

$$p_g = b \cdot \left(\frac{k_c}{b} + k_\phi \right)^n \cdot z_0^n$$

Where the parameters are: b the tyre width, k_c the sinkage modulus from the soil cohesion, k_ϕ the sinkage modulus from the soil friction angle, z_0 the sinkage modulus and n the sinkage exponent.

By knowing the pressure acting on the tyre, calculating the vertical force is just a matter of multiplying the pressure by the contact area. Remembering that the tyre is assumed rigid and that the only deformation comes from the soil, this can be calculated as:

$$A_{cp} = b \cdot l$$

With b the contact patch length which can be calculated as:

$$l = 2 \cdot \theta \cdot R = 2 \cdot \arccos \left(\frac{R-z_0}{R} \right) \cdot R$$

With R the radius of the tyre.

The vertical force then just becomes:

$$W = A_{cp} \cdot p_g$$

3.2.1.2 Plastic ground

Another more commonly adopted approach is to assume the soil as totally plastic. This behaviour is normally regarded as closer to reality. The principle to derive the force equations is still the same, which is to integrate Bekker's pressure-sinkage on the contact patch area. This however is not as straightforward as before and it also results in a longitudinal "compaction force" R_c . The resultant vertical and longitudinal forces are reported below and have been taken from literature [8].

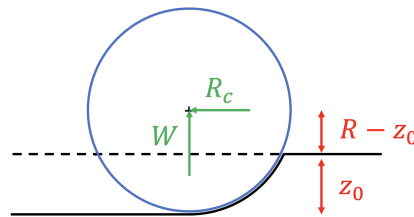


Figure 3.3: Soft ground and rigid tyre - plastic ground

The equations are:

$$W = \frac{b\left(\frac{k_c}{b} + k_\phi\right)\sqrt{2z_0R}z_0^n}{3} (3 - n)$$

$$R_c = \frac{b\left(\frac{k_c}{b} + k_\phi\right)z_0^{(n+1)}}{(n+1)}$$

3.2.2 Soft ground and soft tyres - Stiffness only

The second approach is to consider the tyre to be soft as well instead of rigid. The tyre-soil interaction is modelled by two springs in series. One spring represents the elastic deformation of the tyre, the other one the deformation of the ground. The tyre spring is characterised by its spring stiffness K_t and its deformation δ_t . The ground spring is characterised by its spring stiffness K_s and its deformation z_0 .

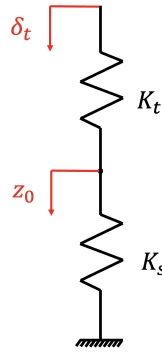


Figure 3.4: Double spring model - tyre and soil

The value of the force in the spring is $F_t = K_t \cdot \delta_t$. Whereas the sinkage dependent force of the soil $F_s(z_0)$ is defined by the plastic soil interaction described above. This can still be seen as a nonlinear spring of stiffness $K_s(z_0)$. Two springs in series can be equivalent to one spring of stiffness K_{eq} and deformation δ_{eq} with the vertical force $W = K_s \cdot z_0 = K_t \cdot \delta_t = K_{eq} \cdot (z_0 + \delta_t)$, hence:

$$W = \frac{K_t \cdot K_s}{K_t + K_s} \cdot (\delta_t + z_0)$$

3.2.3 Soft ground and soft tyres - Stiffness and damping

The concept of the soft ground and tyre modelled as two springs in series can be extended to also include damping both in the tyre and in the soil. It is important to note that “stiffness” and “damping” do not necessarily refer to actual values associated to a linear behaviour. Instead, they refer more generally to the force which depends on the total amount of displacement and velocity. Unlike the previous model, this system has two states, the total deformation and the total deformation velocity.

The equations of equilibrium for elements in series still holds, i.e. the equation $W = F_s = F_t$ remains, but this time another state appears: the deformation velocity. The equilibrium equations are therefore:

$$K_s \cdot z_s + d_s \cdot v_s = K_t \cdot \delta_t + d_t \cdot v_t = K_{eq} \cdot z_{tot} + d_{eq} \cdot v_{tot}$$

Since the input parameters for our simulation will be the total deformation and the deformation velocity, it is possible to calculate the equivalent stiffness and damping as before. However, a different kind of approach will be used in order to calculate the equilibrium point. This is done because the value of z_s

is useful to expand the model further and add other kinds of behaviour such as the compaction force.

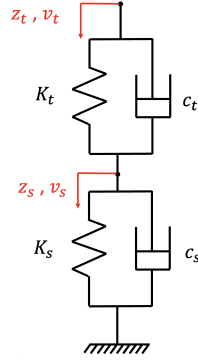


Figure 3.5: Double spring-damper model - tyre and soil

The equilibrium can be calculated by rewriting the previous equation as:

$$F_{g_s} + F_{g_d} = F_{t_s} + F_{t_d}$$

Where the subscript g denotes the quantities relating to the ground and the subscript t is for the quantities related to the tyre. On the same note, s is for forces concerning stiffness (so position dependent) while d is for damping forces (meaning velocity dependent). This can be rewritten as:

$$F_{g_s} - F_{t_s} = F_{t_d} - F_{g_d}$$

The tyre and ground spring forces were always balanced before. Now, taking their difference will result in a “residual” force which will be called F_{res} . Knowing that the ground compression speed is v_g and therefore the tire compression speed will be $(v_{tot} - v_g)$, the previous quantity F_{res} can be used to calculate the ground compression speed. This can be then integrated to find the sinkage z_g . The values of z_g and v_g are used to calculate the vertical and compaction forces. The sinkage can be fed back to then recalculate F_{res} . More detail of how these calculations were actually implemented in the simulation can be found in the next chapters.

Chapter 4

Method and simulations

This chapter deals with the simulation part of the thesis, with the setting of the simulation environment, the choice of the performances studied and their metrics and the definition and implementation of tests.

4.1 Simulation environment

The vehicle simulations were performed using CarSim which is a whole vehicle simulation software developed by the company *Mechanical Simulation*. This was used to simulate the generic vehicle dynamics of the chosen vehicle. Certain interactions however, required more precision in their definition than what are the possibilities within this software. For this purpose, a co-simulation environment was used. The CarSim S-function can be used to get the desired outputs from the simulation and then rewrite some of the quantities as inputs to the simulation. What and how was developed will be shown in detail in this chapter.

The vehicle used for the simulations was of the “Trophy Truck” category. These vehicles are used in high-speed off-road racing, most notably the Baja 1000 [9]. These trucks usually feature rear wheel drive and high horsepower output. Some of the specific parameters of the vehicle used for the simulation, which are generic data coming from CarSim installation, are reported in Table 4.1.

Table 4.1: Vehicle Specifications

| Parameter | Value |
|--------------------------------|----------------------------|
| Total mass | 1626 kg |
| Sprung mass | 1306 kg |
| Front/Rear weight distribution | 51.4% |
| Roll Inertia | 846.6 kg.m ² |
| Pitch Inertia | 1816 kg.m ² |
| Yaw Inertia | 1816 kg.m ² |
| Front suspension type | Independent left and right |
| Unsprung mass front | 140 kg |
| Rear suspension type | Solid axle |
| Unsprung mass rear | 180 kg |



Figure 4.1: 3D model of the truck used in CarSim

4.1.1 Batch Simulations

In order to test many different parameters for the dampers, a MATLAB framework was built. This allowed many tests to be run in sequence and compared to each other afterwards. Each test is defined by a specific road profile, trajectory and damper parameters. The simulations were conducted in discrete time using fixed time-step and a frequency of 2000 Hz.

4.1.2 Damper model

Instead of using the damper model available in the CarSim interface, an external Simulink model was used. This made sure that all the damper models treated in the previous chapters could be implemented in the co-simulation environment. The damper parameters (such as bleed coefficient, offset, slope etc.) can be chosen. Using these, it is possible to determine

the static damper speed-force curve. If a characteristic more advanced like friction or position/frequency dependent damping needs to be modelled, this can be added inside the damper's Simulink model. Whereas this would not be possible on CarSim.

4.1.3 Terrain model

Another thing that the basic CarSim environment is lacking is the definition of different terrain models. This is the reason why the models treated in Chapter 3 had to be developed. All models have been implemented at some point in the simulation framework, but the only one that managed to give seemingly good results was the most complex one i.e. the double stiffness model that includes damping. This takes as an input the variable "TireComp" from CarSim. This variable is defined as the difference between the wheel radius and the distance between the centre of the wheel and the undeformed ground line. In normal usage, since the ground is assumed to be perfectly stiff, this corresponds to the tyre deformation, hence the name "TireComp" (short for Tyre compression). Multiplying this value by the radial stiffness of the tyre will result in the vertical force. It is worth noting that this value must be saturated to be only positive since the vertical force exerted by the tyre can only be positive.

Since the normal CarSim tyre model does not take into account the radial damping, the compression velocity is not something that can be obtained directly. Instead, a discrete derivative is applied to the "TireComp" signal in order to get the tyre compression velocity. This is appropriately named "TireCompV". Another input signal for the tyre-soil interaction model is the "Surface". This contains a number which identifies which soil type each wheel is running on depending on the position of the car along the track. The surface signal must be fed into the various look-up tables to determine which soil characteristics will be selected.

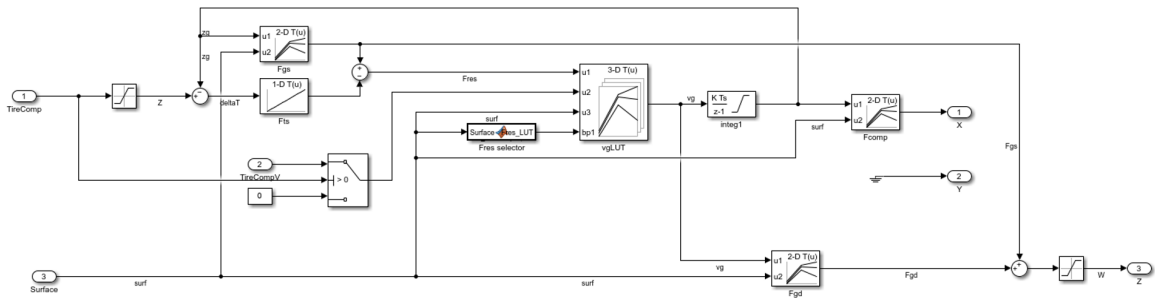


Figure 4.2: Terrain model made in Simulink

A quick overview of the inner workings of the Simulink model will be made in the following paragraphs.

The “TireComp” signal (input port 1) is firstly saturated to ensure that no negative tyre force is applied. To this, the most recently calculated z_g (ground deformation) is subtracted. As seen in chapter 3.2, this results in the tyre deformation “deltaT” that can be used to calculate the tyre spring force. In the model, this is done by the look up table called “Fts”. The z_g signal is also used to calculate the ground spring force.

The ground force is subtracted to the tyre spring force to calculate the residual force F_{res} . This is used to calculate the ground deformation speed v_g when combined with the total deformation velocity. It’s worth noting that the “TireCompV” signal is set to zero when the tyre is not in contact with the ground.

The ground deformation speed v_g is used to calculate the soil damping force F_{gd} . This signal is also integrated to compute the ground deformation. With this, the ground spring force F_{gs} is calculated. Summing ground spring and damping force F_{gd} gives as a result the total vertical force to be applied on the tyre. This is again saturated to only assume positive values. The ground deformation is also used to compute the longitudinal compaction force “Fcomp”.

An extensive use of look-up tables can be noticed in this model. This was done to reduce the number of calculations needed during simulation time, in order to decrease the computation time for each simulation. The contents of

"Fgs" and "Fcomp" both come from the soil equations described in Chapter 3.2. The tables "Fts" and "Fgd" both describe linear behaviours but have been implemented in this way for ease of future modification. "VgLUT" computes the value of ground compression velocity that balances the forces in the system. The pre-computation of these values ensures that the simulation runs smoothly.

4.2 Metrics

Testing is one of the most important phases when optimising vehicle performance. Different testing scenarios are used to evaluate the vehicle's performance in different environment. The behaviour of the vehicle in these scenarios can be numerically assessed using different metrics.

The unevenness of the road and the harsh changes in the elevation profile of off-road tracks result in a lot of chassis movement. Off-road engineers focus on reducing the accelerations of the vehicle's sprung mass and their effects on the driver and minimising the amplitude of dynamic tire-ground loads, thus maximising terrain-friendliness and ride safety.

Choosing the right metrics to optimise performance in a given scenario was a key point during this thesis. The vehicle's performance is evaluated by studying its response using some of these metrics depending on what is being studied.

The maximum damping force is a metric of primary importance. Its value depends on the damping curve and should remain lower than a critical value F_{max} .

Similarly, the maximum damping velocity also depends on the damping curve and cannot be higher than a certain value v_{max} (around 7 m/s).

It can also be interesting to look at the damper displacement, especially when there are jacking-up or jacking-down responses.

The human body is not sensitive to speed but acceleration. Thus, it is necessary to tackle the maximum vertical acceleration of the chassis is subjected to when it comes to ride comfort and ensure its maximum value

stays reasonable.

The damper being a mechanical component subject to high force variations, it is also subject to overheating. It is important to ensure that the damper temperature remains under a certain value, typically around 150 °C, to prevent the melt of rubber components.

Coupled to the longitudinal movement of the vehicle, the vertical road excitation induces pitch, heave and roll. The pitch, roll and heave angles, as well as the pitch and roll rates need to be studied.

The roll, pitch and heave responses can also be studied in the frequency domain. This was done by analysing the power spectral density of their signal.

For the jump and the bump absorption test scenarios, the truck is subjected to a single perturbation. It is interesting to observe when the vehicle settles around its initial steady state, i.e. to study the settling time.

The road unevenness also implies that, due to the many bumps and ditches present on the road, the wheels will not always keep contact with the ground, depending on the vehicle speed, the road profile and the damper settings. This is particularly important during competition as a floating tyre will not be able to exert longitudinal force to move forward. For this reason, the “airtime events” were defined. An airtime event begins with a “Take-off” which is the first instant when all the tyre loose contact with the ground. The airtime event lands with a “Landing”. This is defined as the first instant after a Take-off when all four wheels regain contact with the road surface. These needed to be specified in order to calculate the “airtime percent” parameter, which will just be the percentage of the time during the run spent between take-off and landing. This quantity was defined in this way in order to capture the fraction of the time that the vehicle spends in an "unsettled" state. Other methods to calculate the same quantity were considered. for example another way this could have been defined was by calculating the percentage of time spent in the air by each single wheel. Both methods were tested and the difference wasn't particularly striking. The first method was chosen since it puts a higher focus on the whole-vehicle motion.

Another important parameter to maximise grip is the load variation on the tyres. It is important to keep the load as equally distributed as possible

on all four wheels to maintain the balance of the car. Therefore the “Load Variation” metric was created. This is defined as the average value throughout the whole run of the standard deviation of the load between the four tyres. The idea behind this is to minimise the load transfer between the tires in order to maximise grip. The standard deviation allows to quantify the load variation. Taking its average value among all time samples can show how much load variation happens throughout the whole run. Since when the vehicle is off the ground the load is zero on all four wheels, this could skew the results and artificially reduce the load variation of test runs with high airtime. Because of this, the calculation of this quantity is limited to the instances where at least one tyre is on the ground. The formula for this quantity is shown below:

$$LV = \frac{1}{n} \sum_{i=1}^n std(F_i^{fl}, F_i^{fr}, F_i^{rl}, F_i^{rr})$$

Where *LV* stands for *Load Variation*, F_i^{nn} indicates the force at instant i of the tyre nn (front left, rear right etc.). It's worth noting that n is not the whole simulation time since the airtime will be excluded.

Studying the yaw rate gives the steering response, which is necessary in case of a steering manoeuvre, since the yaw rate is set in relation to the steering angle.

When cornering, a load transfer due to lateral acceleration happens between the left and right side of each axle. It is interesting to look at what ratio of the total load transfer happens on each axle and how this changes dynamically throughout a whole cornering manoeuvre.

4.3 Scenarios

Off-road tracks differ from usual testing tracks, that often are on circuits or airfields. Off-road tracks have very specific terrains while on-road tracks are made of asphalt. In off-road, it can be mud, sand, snow, etc. The track profile is also very different between on-road and off-road. On-road tracks are usually straight or slightly curved roads while during off-road testing, many different profiles are tested, some very peculiar, in order to be the closest to real off-road conditions. It can be a series of bumps, ramps, axle-twisting segment or also uneven road segments (dunes).

Since off-roading is such a broad term, evaluating the vehicle performance in every possible scenario would be impossible. Moreover, each scenario can also be evaluated using a lot of different metrics, making the combinations endless. Hundreds of scenarios can be evaluated when it comes to off-road, and the reader might realise that it is fundamentally impossible to conduct all of them and that choices are to be made when investigating off-road suspensions. Considering the scope of this master's thesis, it has obviously not been possible to tackle all of them. The focus was made on the most intuitive ones as well as the ones that seemed the most relevant. In this section, all the scenarios evaluated later in this thesis are presented.

4.3.1 Chassis stability

One of the most important things when it comes to a suspension systems is to isolate the chassis from the vibrations of the unsprung masses. This is done to optimise the comfort of the vehicle as when too many vibrations are being transmitted to the driver it may cause fatigue. Clearly then, this is not just important in passenger cars but also for competitions where extensive driving hours are necessary, like the Dakar for instance. That said, the movement of the sprung mass needs to be controlled to also avoid having heavy oscillations and high angles in roll and pitch. This results in a tricky problem where a lot of parameters are involved. This requires a careful study to reach a good behaviour of the suspension.

From the metrics listed in section 4.2 the ones which were chosen to evaluate the chassis stability performance are the following:

- Damping force, damping velocity and damper displacement
- Airtime
- Tyre load variation
- Heave, roll and pitch
- Pitch and roll rates

Damper forces, velocities and displacements are analysed to make sure that the damper are operating in a realistic window. Heave, roll pitch and their respective derivatives are taken into account to measure the dynamic behaviour of the chassis. Lastly, airtime and tyre load variation are a good indicator of

how much grip is available.

Two optimisation scenarios have been created to explore the vehicle's performance under different conditions. Firstly, the low-speed scenario set at 40 km/h replicates rock crawling environments. This constant speed test is chosen for its simplicity, since it enables the use of linear model approximations of the chassis for initial studies. Moreover, the selected speed is calibrated to excite the pitch natural frequency of the vehicle, striking a balance between simulation duration and realism, ensuring efficient analyses while preserving critical dynamics.

Conversely, the high-speed scenario, set at 80 km/h, mimics dune riding conditions. Despite the higher speed, this scenario features fewer road irregularities, carefully designed to offer a challenging yet manageable terrain. Considerable effort was dedicated to finding this delicate balance, as too challenging conditions introduce randomness and instability into the results, while overly simplistic scenarios render damper performance less influential.

The road profile itself was built starting from white noise and then applying a band pass filter to choose the cut-off frequency for maximum and minimum frequency. The white noise was created with a random number generator and a numerical seed that was kept constant to ensure repeatability. The seed was the same for the tests at 40 and 80 km/h, for this reason the first 150m of the high speed test look very similar in shape to the low speed test. The main difference between the two is the amplitude of the obstacles.

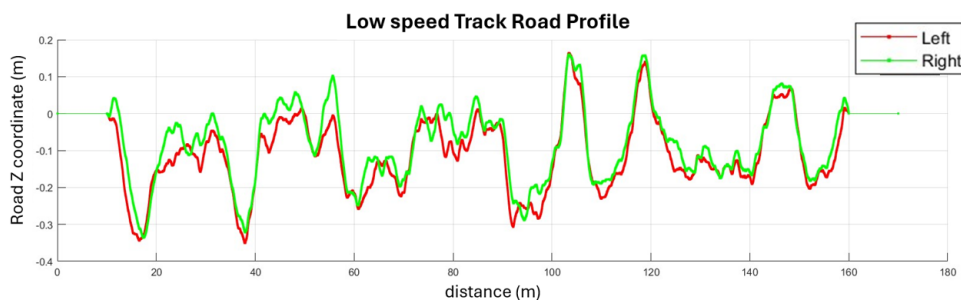


Figure 4.3: Road profile - low-speed (40 km/h) chassis stability test

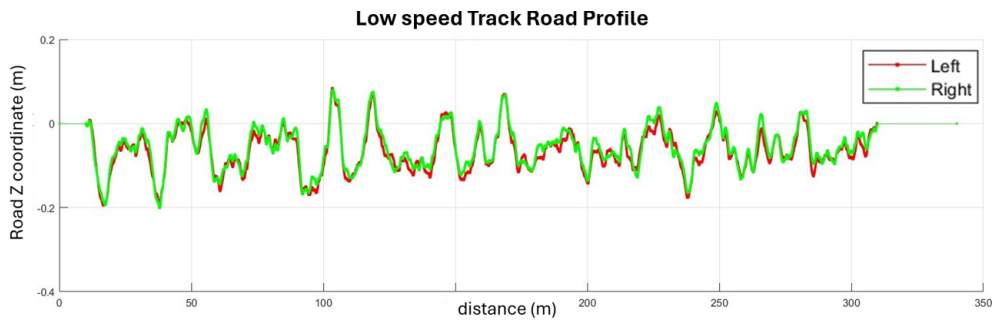


Figure 4.4: Road profile - high-speed (80 km/h) chassis stability test

4.3.2 Bump Absorption

The unevenness of the road entails that the vehicle often faces particular road profiles such as bump and ditches. An important performance is then be the “bump absorption” of the vehicle. An off-road truck must be able to have an adequate response to a bump, which might occur frequently on an off-road terrain.

The bump absorption test is used to evaluate the response of the vehicle to a single bump of medium amplitude. It is a very important test since this kind of profile occurs quite often in an off-road environment. The bump used is 0.15 m tall, 3 m long and occurs 5 m after the start of the run (see Figure 4.5). The dimensions come from visual research on existing off-road races.

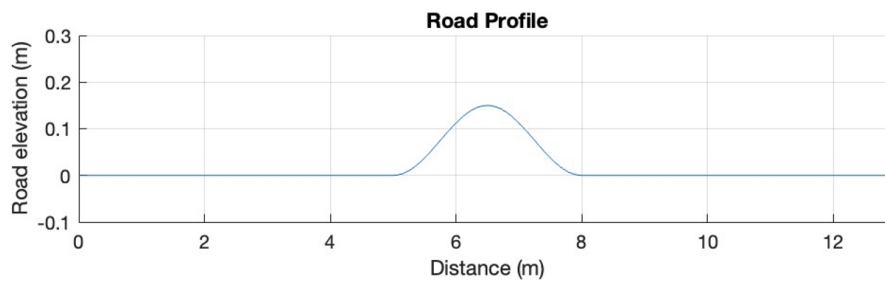


Figure 4.5: Road profile - bump absorption test scenario



Figure 4.6: 3D visualisation of the bump absorption test on CarSim

The metrics chosen to evaluate the bump absorption performance are the following:

- Damping force, damping velocity and damper displacement
- Damper temperature
- Heave, pitch and pitch rate
- Settling distance

4.3.3 Jump

When off-roading, it is not uncommon to encounter either big drops or for the road to assume a ramp-like shape. If taken with enough speed this will result in the car jumping. A lot of competitions often also add jumps to their tracks or routes to increase the spectacle of their racing. It is important that the vehicle behaves correctly during this kind of scenarios since there are usually very high forces involved. A bad setup could mean not only that the response is subpar but also increase the risk of breakage of the car or, even worse, injury of the driver.

The jump test is used to evaluate the response of the vehicle to a single jump of medium amplitude. The ramp is 0.8 m tall, 5 m long and occurs 5 m after the start of the run. The dimensions of this jump correspond to the ones of the Stadium SuperTruck racing series in Australia [10].

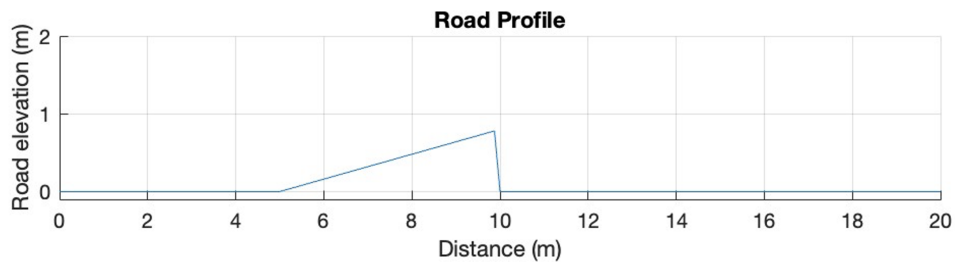


Figure 4.7: Road profile - jump test scenario



Figure 4.8: 3D visualisation of the jump test on CarSim

The metrics chosen to evaluate the jump performance are the following:

- Damping force, damping velocity and damper displacement
- Damper temperature
- Pitch and pitch rate
- Settling distance

4.3.4 Acceleration and braking

Although the scenarios discussed previously tackle specific off-road profile, off-road vehicles are still supposed to have good responses to more classic scenarios (in the sense that those performances also apply to on-road cars). That said, the vehicle must be able to accelerate and brake decently.

The test for the acceleration of the car is useful to determine the vehicle's behaviour in dynamic manoeuvres. As opposed to the previous cases, the

excitation in the dampers is mostly in the very-low-speed region. There is usually a balance that needs to be found in the setup so that the suspension is soft enough to ensure chassis stability over bumps and irregularities, but also stiff enough to maintain a good attitude during acceleration manoeuvres.

The car is travelling in a straight line on flat ground while following a specific speed profile. For the acceleration part, the speed profile has been chosen in order to let the car go full throttle starting from standstill. The profile displayed on Figure 4.9 is the reference profile that the driver is asked to follow, not the actual speed. Once the speed of 100 km/h has been reached, there is a small window of travelling at the same speed to let the vehicle settle. After that, the braking manoeuvre begins. This was designed to keep the vehicle on the grip limit while still making sure that the ABS system does not kick in. This would create a lot of vibration which would influence the dynamics of the vehicle and make the results a lot harder to read.

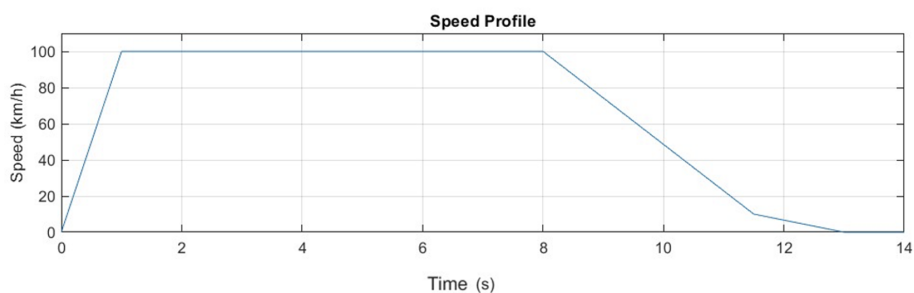


Figure 4.9: Speed profile - acceleration and braking test scenario

The metrics chosen to evaluate the acceleration and braking performance are the following:

- Damper displacement
- Pitch and pitch rate

4.3.5 Steering

Similarly as for acceleration and braking, the vehicle must be able to steer properly and that aspect thus needs to be studied.

Making sure that the behaviour of the vehicle is good enough during steering manoeuvres is important for both performance and safety purposes.

For this reason it was deemed relevant to perform an optimisation to see which damper characteristic best suit the car in order to maximise the performance in this scenario.

In this section the optimisation focuses on the steering behaviour. To do this, two different scenarios are investigated: the first one is a step steer manoeuvre up to 60 degrees for the steering wheel angle at 60 km/h. This is useful to study the transitional behaviour between two different steady states. The second test is a double lane change, performed at the speed of 100 km/h to investigate a much more dynamic case.

The metrics chosen to evaluate the steering performance are the following:

- Roll, roll rate and yaw rate
- Load distribution

4.3.6 Acceleration and braking comparison

The previous scenarios discussed in this section will all result in different optimal damper settings. Some of these (like chassis stability, bump absorption and jump) are very particular cases, therefore they may result in quite extreme setups. Even if the vehicle has been tuned specifically for one of these scenarios, it is supposed to be able to offer a decent behaviour during normal driving manoeuvres. For this reason, the acceleration/braking test is performed not only with the resulting optimal parameters from the optimisation process, but also with the resulting setup of the optimisation process of chassis stability and jump.

The test's environment and manoeuvre are the exact same ones as conducted before in Section 4.3.4. The values of the damper parameters used for the chassis stability setting are the ones listed in Table B.1 (high-speed) and the ones used for the jump setting are the ones listed in Table D.1 (medium-speed).

4.3.7 Steering comparison

Similarly to the process conducted for the acceleration and braking comparison, the same comparison is done for the steering behaviour. The test conducted is the double lane change explained in Section 4.3.5. The double lane change test is performed not only with the resulting optimal parameters

from the optimisation process, but also with the resulting setup of the optimisation process of chassis stability and jump. The values of the damper parameters used for the chassis stability setting are the ones listed in Table B.1 (high-speed) and the ones used for the jump setting are the ones listed in Table D.1 (medium-speed).

4.3.8 Influence of friction

The modelling and implementation of the internal friction of the damper has already been discussed previously in this thesis in section 2.3.2. It is deemed interesting to study its influence on the behaviour of the damper. Two tests have been conducted in order to determine its influence on the damping performance: the bump absorption test at medium speed (60 km/h) and the jump test at medium speed (60 km/h). For the bump absorption test, the comparison is made between the regular damper with internal friction and the regular damper without. For the jump test, it is made between the damper with the blow-off and high-speed choke valves with internal friction and the same damper without. This study can thus show if the friction has an influence on the regular damper, the damper with blow-off and high-speed-choke or none.

4.3.9 Influence of soft soil

The influence of having a non-rigid driving surface was explored using the most advanced model shown in Chapter 3.2, i.e. the model in Section 3.2.3. The type of soil that was investigated was dry sand. Since the high-speed chassis stability test presented in section 4.3.1 is meant to represent dune riding (it represents the dunes that can be found in off-road competitions such as the Baja 1000 or the Dakar), it was deemed appropriate to use that one. The damper parameters used were the optimal ones for the corresponding rigid-surface scenario (listed in Table B.1).

4.4 Optimisation process

In the previous section the optimisation scenarios were covered for each specific case. This section instead is going to tackle the process with which each optimisation setup was obtained.

While all scenarios were tackled with slightly different approaches due to their specific quirks, one thing that unites all optimisation processes is that no strict mathematical method (e.g. gradient descent) was used to obtain the final result. While defining a cost-function and minimum search method would have been possible (albeit time consuming and computationally intensive), it was deemed more useful to conduct simple parameter sweeps. This "manual" approach allowed to get a bit more insight into how each parameter affects the final behaviour. Being able to investigate the intermediate results, as opposed to just getting a final optimal behaviour, was useful to get a greater understanding of what and how certain parameters are more important than others.

The parameters at stake are the following:

- Bleed valve coefficient ($\text{N}\cdot\text{s}^2/\text{m}^2$)
- Poppet valve offset (N)
- Poppet valve slope ($\text{N}\cdot\text{s}/\text{m}$)
- Blow-off valve coefficient ($\text{N}\cdot\text{s}^2/\text{m}^2$)
- Blow-off valve offset (N)
- High-speed-choke valve coefficient ($\text{N}\cdot\text{s}^2/\text{m}^2$)

As explained in chapter 2.3.1.2 the bleed valve coefficient is a parameter that lumps together many different parameters like fluid density and orifice area. Since it's the parameter that relates the square of the speed to the force, its units will be $\text{N}\cdot\text{s}^2/\text{m}^2$. The poppet valve offset just represents the preload of the spring of the poppet valve and it's measured in N since it's just a force. The slope instead is measured in $\text{N}\cdot\text{s}/\text{m}$.

No optimisation was made for the acceleration/braking and steering comparisons as well as for the influences of soft soil and friction.

4.4.1 Chassis stability

The optimisations for both the 40km/h and the 80 km/h scenarios referenced in section 4.3.1 were conducted using an equivalent process. It commences with the selection of two damper curves: one soft and one stiff. The soft curve entails lower values of bleed, offset, and slope, contrasting with the stiffer

counterpart. Every single combination of these curves in compression and rebound across both front and rear axles is systematically tested, yielding a parameter sweep of 16 runs. This iterative process is repeated, with subsequent iterations featuring curves positioned closer to each other. Furthermore, a sensitivity analysis is undertaken on each parameter to elucidate the extent of influence exerted by minor parameter adjustments on the vehicle's behaviour.

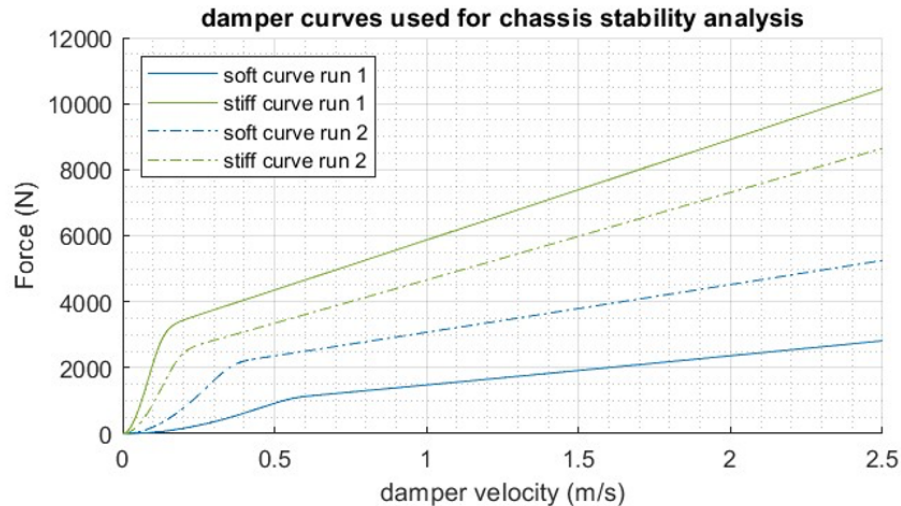


Figure 4.10: Damper curves used for the chassis stability analysis

The curves shown in figure 4.10 are obtained by changing the following parameters:

- Bleed valve coefficient (compression and rebound, front and rear)
- Poppet valve offset (compression and rebound, front and rear)
- Poppet valve slope (compression and rebound, front and rear)

4.4.2 Bump Absorption

Three optimisations have been conducted, each involving a different speed: low speed (30 km/h), medium speed (60 km/h) and high speed (90 km/h).

Each scenario has been tested for a regular damping setting, involving bleed and poppet valves, as well as for a damping setting involving blow-off and high-speed choke valves. The latter configuration aims to find the best

response for a damping force inferior to 10 000 N.

During the optimisation process, the following parameters have been tested and optimised for both the front and rear axle:

- Bleed valve coefficient (compression and rebound)
- Poppet valve offset and slope (compression and rebound)
- Blow-off valve coefficient and offset (compression)
- High-speed-choke coefficient (rebound)

The optimisation has been executed by conducting step-by-step sweeps of the above parameters until the response is considered optimal.

4.4.3 Jump

The optimisation process is the exact same as for the bump absorption scenario: three different speeds are tested, as well as two damper settings (with and without blow-off and high-speed choke valves). The optimised parameters are the same (bleed valve coefficient (compression and rebound), poppet valve offset and slope (compression and rebound), blow-off valve coefficient and offset (compression) and high-speed choke coefficient (rebound)).

4.4.4 Acceleration and braking

For this kind of manoeuvre, the dampers are almost exclusively excited in the low-speed region i.e. below 0.1 m/s. This makes the optimisation process for the dampers much quicker since there is little concern for the high-speed region. For this reason, a full sweep was performed over the value of the bleed valve coefficient, ranging from very low to very high values. A further analysis was then conducted to determine the influence of having different damping curves in the front and in the rear.

4.4.5 Steering

Akin to what was observed during the tests conducted for evaluating the acceleration performance, the dampers only work in the low-speed region while the vehicle is steering. This means that the focus of the parameter sweeps can be concentrated exclusively on the bleed coefficient.

Chapter 5

Results

In this section all of the results gathered from the simulation environment will be shown. These are divided in different sections depending on what the objective was.

5.1 Chassis stability

With the optimisation setup and scenario explained in the previous section, two damper configurations were obtained that represent the ideal setup for rock crawling (40 km/h) and dune riding (80 km/h). The optimal parameters are displayed in the appendix in table B.1. It can be noticed that the setup is quite similar in almost all parameters. The biggest difference is in the front axle bleed valve coefficients. While both setups will result in a jacking down behaviour, this is a lot more evident in the rock crawling setup. Other graphs about this test runs are available in the appendix B.

5.1.1 Rock Crawling Results

During the optimisation process, particular attention was put into the maximum damper forces and speeds as well as the grip metrics. Along with the results from the optimal setup, two other sets of results are added to provide a comparative baseline; these refer to sub-optimal solutions that are either too soft or too stiff. It can be noticed from Table 5.1 that the optimal setup minimises the airtime while still keeping the maximum force within reasonable values.

Table 5.1: Numerical results - low-speed (40 km/h) chassis stability test

| | Soft Setup | Optimal Setup | Stiff Setup |
|--------------------------------|------------|---------------|-------------|
| Maximum damping velocity (m/s) | 4.22 | 3.67 | 2.65 |
| Maximum displacement (m) | 0.25 | 0.20 | 0.11 |
| Maximum damping force (N) | 4,760 | 9,503 | 12,600 |
| Airtime (%) | 20.7 | 16.7 | 20.9 |
| Load Variation (N) | 3,540 | 2,779 | 3,344 |

Other parameters were also considered when choosing the optimal setup. Some of the most significant ones are shown in the graphs below, starting with the pitch-roll envelope represented in Figure 5.1. Marked with asterisks is the median value of roll and pitch angles throughout the run, this is useful for example to determine if the car has a generally squatting or diving behaviour. This can happen if one of the axles has an asymmetric behaviour in compression and rebound which will result in the axle progressively extending or compressing throughout the run. Marked with the circle instead is the standard deviation of the roll and pitch signal which provides a good measure of how much the vehicle is oscillating. Finally the lines that enclose the areas are the envelope of the pitch and roll angles signal throughout the whole run.

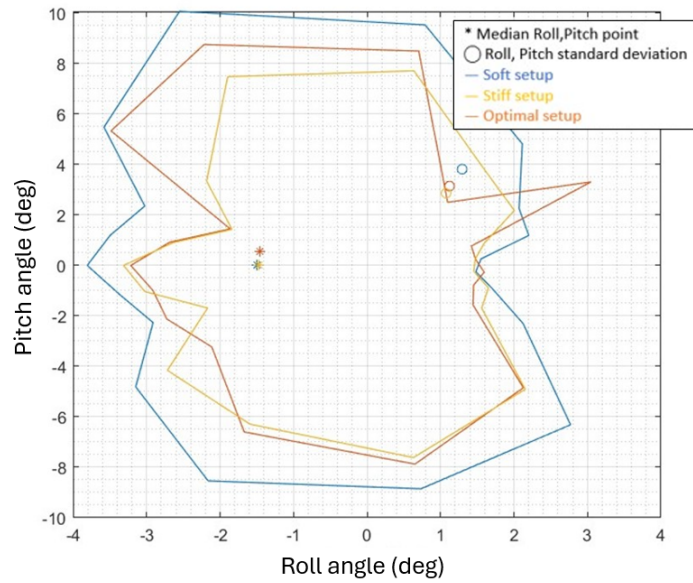


Figure 5.1: Pitch-roll envelope - low-speed (40 km/h) chassis stability test

While the stiff setup is the one that minimises the area inside the envelope, the optimal setup is still able to provide a good behaviour as it keeps the roll angle between plus and minus 3 degrees and the pitch angle between plus and minus 8 degrees.

Finally, the behaviour in pitch and roll rate is studied. From these two graphs shown in Figures 5.2 and 5.3 it is clear that even if the minimum values are obtained with the stiffer damper curves, the optimal one can get quite close to it while also keeping other advantages such as lower airtime and damper forces.

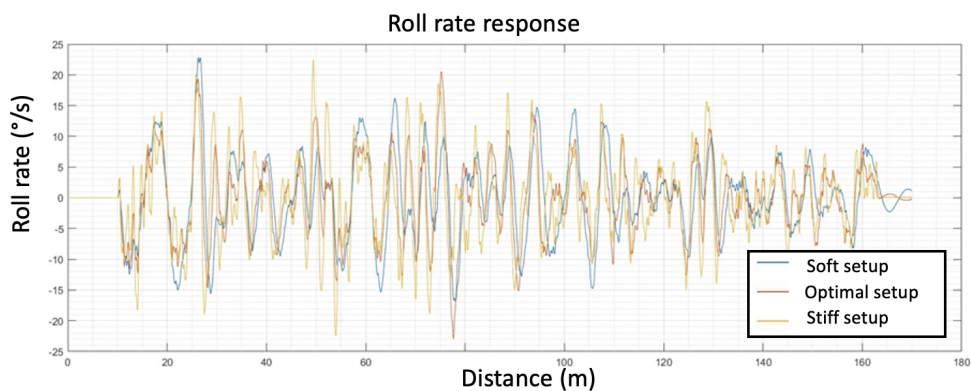


Figure 5.2: Roll rate - low-speed (40 km/h) chassis stability test

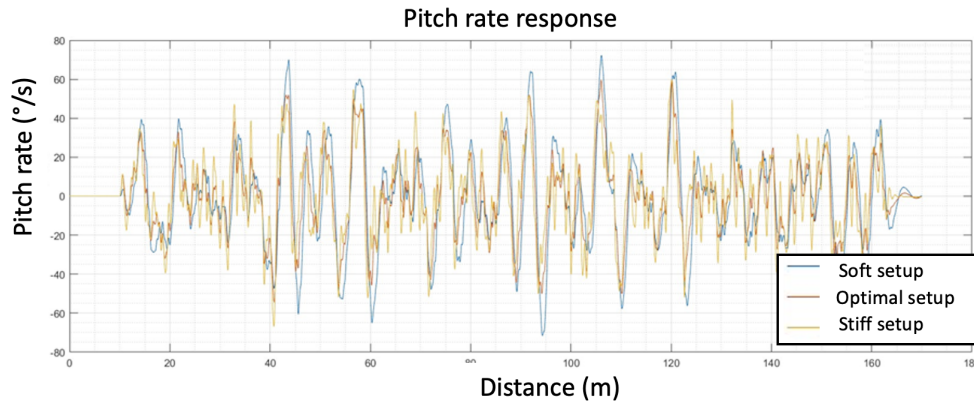


Figure 5.3: Pitch rate - low-speed (40 km/h) chassis stability test

5.1.2 Dune riding Results

Similarly as how the analysis was conducted before, one of the most important parameters that was taken into account was the grip metrics. The optimal values were chosen to keep this values as low as possible while also keeping the maximum forces under 10,000 N. These values are all shown in Table 5.2 along a soft and stiff setup like before.

Table 5.2: Numerical results - high-speed (80 km/h) chassis stability test

| | Soft Setup | Optimal Setup | Stiff Setup |
|----------------------------------|------------|---------------|-------------|
| Maximum damping velocity (m/s) | 4.86 | 4.17 | 3.35 |
| Maximum damping displacement (m) | 0.28 | 0.17 | 0.15 |
| Maximum damping force (N) | 4,959 | 8,397 | 13,055 |
| Airtime (%) | 32.8 | 25.8 | 35.4 |
| Load Variation (N) | 2,991 | 2,614 | 3,263 |

As done before, the analysis can be continued by looking at the pitch-roll envelope shown in Figure 5.4. The difference between the cases here is quite striking. The stiff and optimal setup are quite close in terms of each other in the pitch values as both have extreme values between 6 and -4 degrees. The soft setup has lower extreme values as it goes from -2 to 5 degrees. The situation inverts when focusing on the roll angle as now the soft setup is the worst performing one, going from -2 to 2.5 degrees, as opposed to the optimal setup which always manages to stay below 1 degree of roll in both directions.

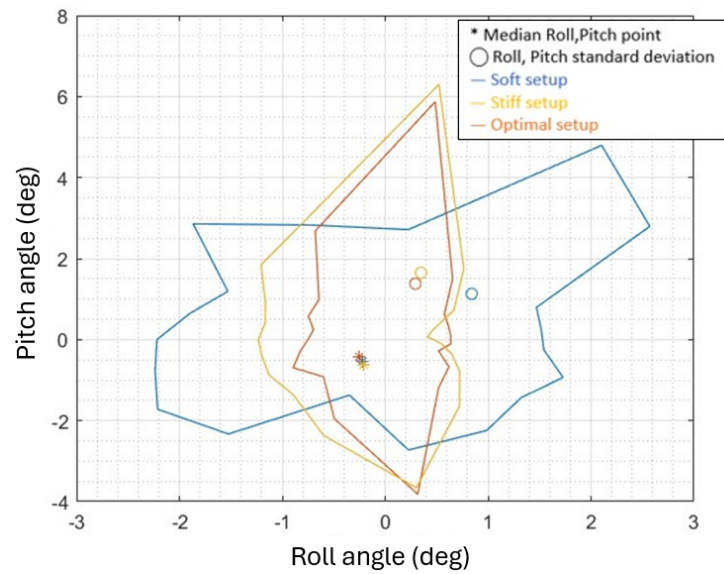


Figure 5.4: Pitch-roll envelope - high-speed (80 km/h) chassis stability test

What was noticed in the pitch-roll envelope graph can also be seen in Figures 5.5 and 5.6 which displays the pitch and roll rates. While the blue curve seems to perform best in pitch dynamics it is considerably worse when it comes to roll rate performance. Also in this case the optimal setup is a great compromise between the two edge cases.

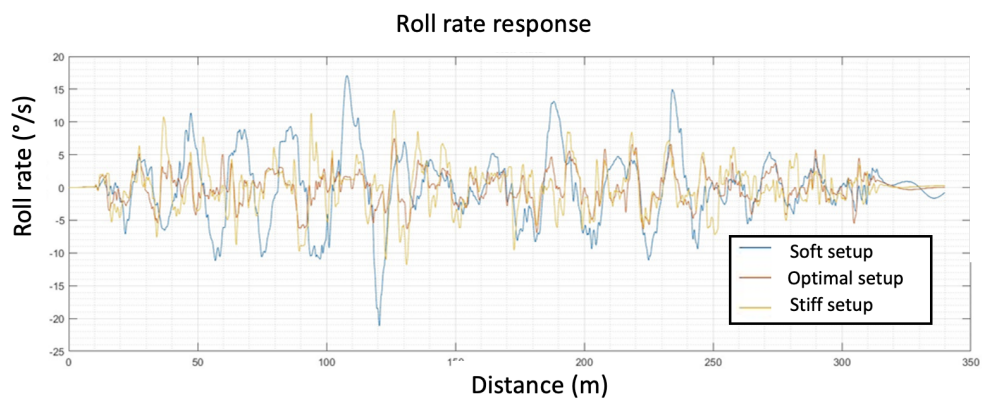


Figure 5.5: Roll rate - high-speed (80 km/h) chassis stability test

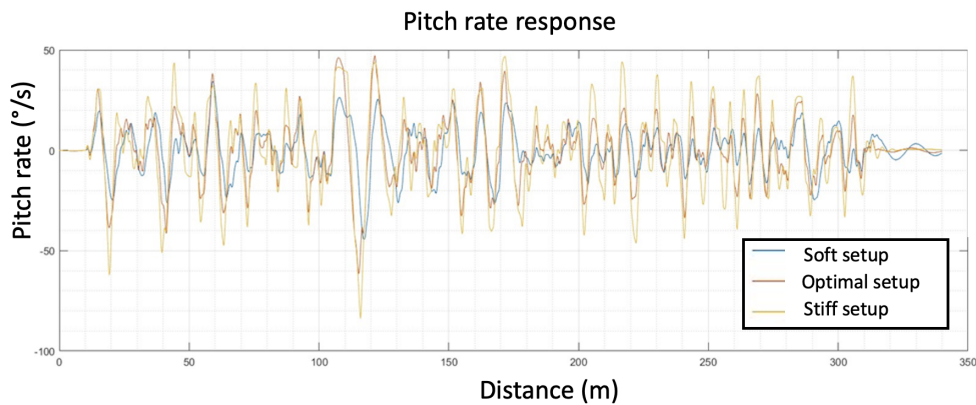


Figure 5.6: Pitch rate - high-speed (80 km/h) chassis stability test

5.2 Bump Absorption

After a careful optimisation for both front and rear axles, and for compression and rebound, the parameters listed in Table C.1 have been selected. The values of the numerical metrics defined previously are displayed in Table C.2. The graph results are displayed in the Appendix C.

Figures C.1, C.6 and C.11 represent the heave response, figures C.3, C.8 and C.13 the pitch response, figures C.4, C.9 and C.14 the pitch rate and figures C.2, C.7 and C.12 the vertical acceleration of the chassis. Figures C.5, C.10 and C.15 represent the response of the vehicle to the bump, with its heave and pitch motions.

When looking at Figure 5.7, it can be observed that the damper velocities reached are quite similar for both damping settings for the low-speed test (30 km/h). They are mostly concentrated in the $[-0.2 \text{ m/s}; 0 \text{ m/s}]$ interval, for both front and rear axle.

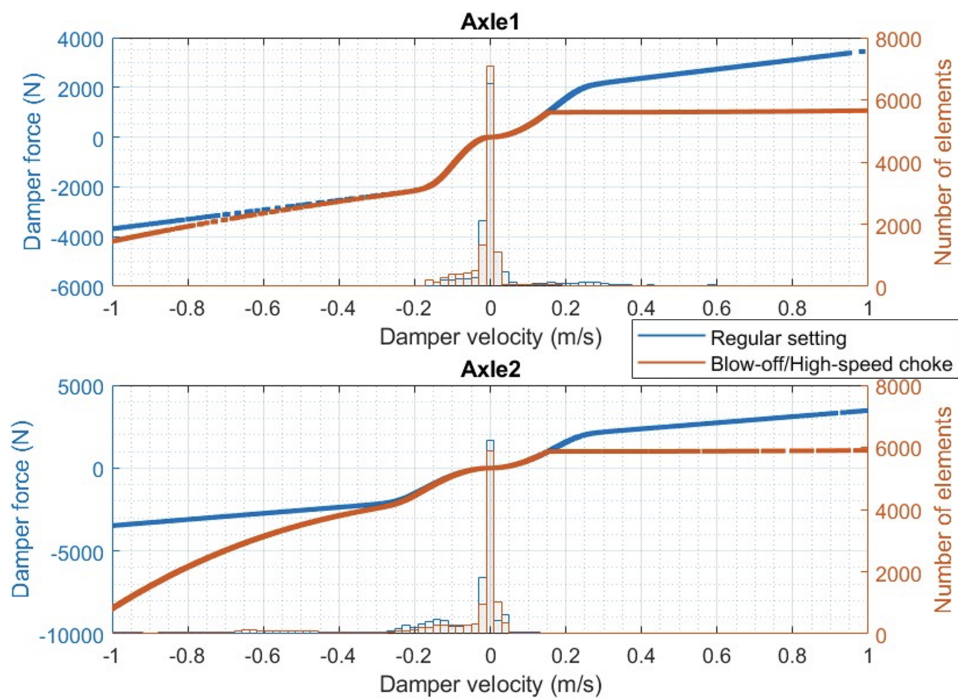


Figure 5.7: Damping curves - low-speed (30 km/h) bump absorption test

Figure 5.8 shows that the damper velocities reached are quite similar for both damping settings for the medium-speed test (60 km/h). They are mostly concentrated in the $[-0.2 \text{ m/s}; 0.1 \text{ m/s}]$ interval for the front axle and in the $[-0.4 \text{ m/s}; 0.1 \text{ m/s}]$ interval for the rear axle.

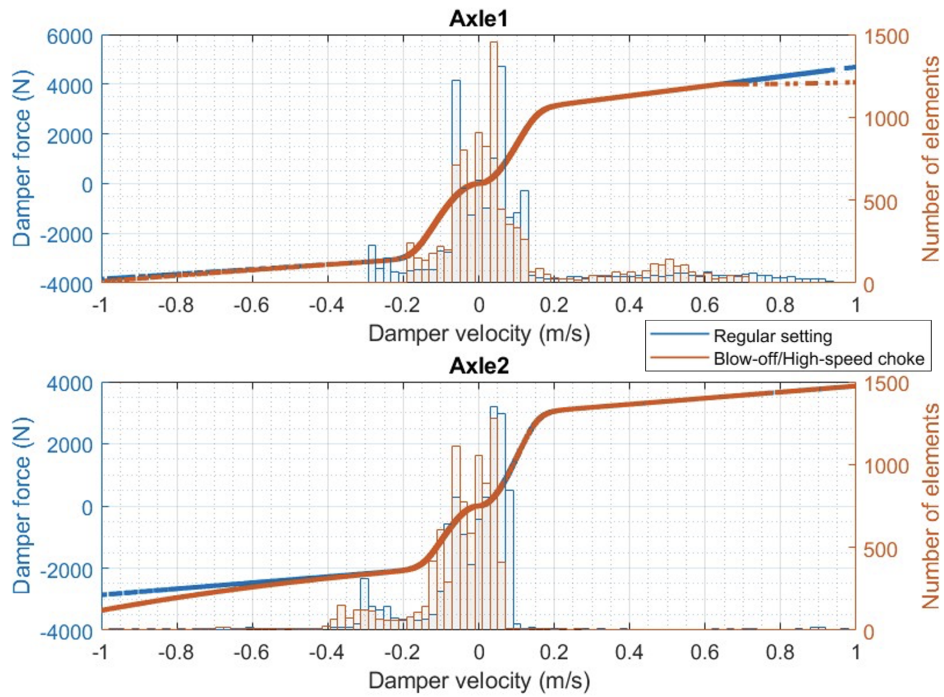


Figure 5.8: Damping curves - medium-speed (60 km/h) bump absorption test

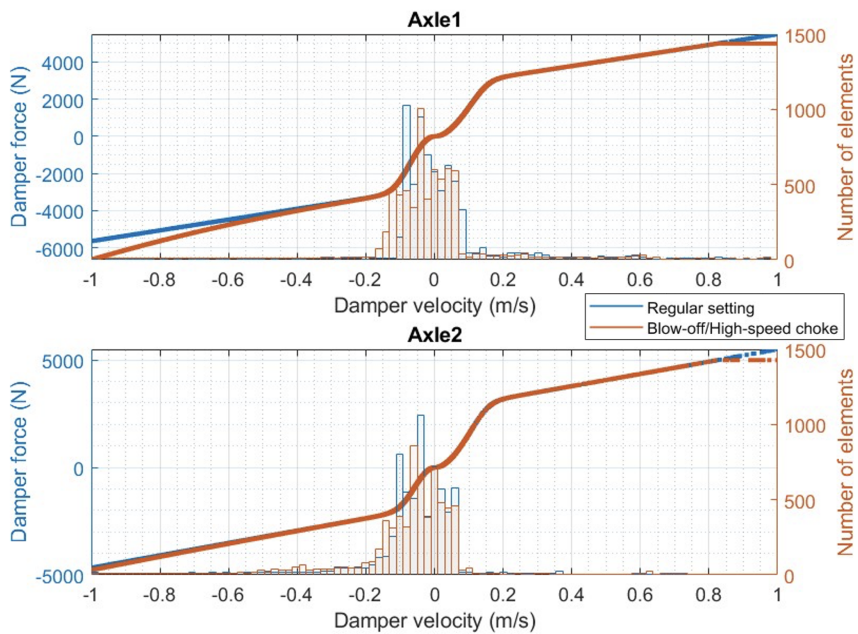


Figure 5.9: Damping curves - high-speed (90 km/h) bump absorption test

When looking at Figure 5.9, it can be observed that once again the damper velocities reached are quite similar for both damping settings for the high-speed test (90 km/h). They are mostly concentrated in the [- 0.2 m/s ; 0.1 m/s] interval for both front and rear axles.

For the medium-speed (60 km/h) test, the maximum damping force is equal to 13,263 N for the regular damping setting. With the introduction of the blow-off and the high-speed choke valves, this value is reduced to 9,625 N. It is more than double the value of the low-speed test. The maximum damping velocity has increased from 7.5 m/s to 7.9 m/s and is slightly above the critical value for both settings. The maximum vertical acceleration of the chassis has decreased with the blow-off/high-speed choke setting but is still around 3 g for both settings. The maximum pitch rate is around 30 °/s for the simplest setting and 35 °/s for the most complex one, which is less than for the low-speed test. The pitch envelope has also decreased but the damper temperature has increased and is now around 92 °C, in comparison to the low-speed test. Unlike the low-speed test, the benefit given by the setting with the blow-off and high-speed choke valves in comparison to the regular setting is not that visible. Admittedly, the damping force has been reduced by around 4,000 N and the maximum heave by a couple of centimeters, but it has not been possible to lower the value of the damping velocity below the critical value, and important metrics such as the maximum pitch rate and the pitch envelope have increased, as well as especially the settling distance, which increased by 35 m, that is to say more than 40%.

Concerning the high-speed test, for the regular damper setting, the damping forces reaches 20,000 N, with a maximum damping velocity of 6.1 m/s and a maximum vertical chassis acceleration of 4.3 g. The pitch envelope is lower than for the 60 km/h scenario (now less than 3°) and the maximum pitch rate is slightly above 32 °/s. The main observation point concerning the damper with the blow-off and the high-speed choke valves is that the force has been reduced from 20,011 N to 9,092 N, which is a decrease of 55%. This decrease has been possible without increasing too much the maximum damper velocity (now 7.3 m/s, i.e. at the limit of the critical value) and with the decrease of the maximum vertical chassis acceleration to only 2.7 g. The pitch response remains the same in terms of amplitudes and maximum values. However, the settling distance increased from 120 to 150 meters, i.e. an increase of 25%.

5.3 Jump

The parameters listed in Table D.1 are the parameters that have been selected after careful optimisations for both front and rear axles, and for compression and rebound. The values of the numerical metrics defined previously are displayed in Table D.2. The graph results are displayed in the Appendix D.

Figures D.1, D.4 and D.7 represent the pitch response, while figures D.2, D.5 and D.8 represent the pitch rate. Figures D.3, D.6 and D.9 represent the response of the vehicle to the bump, with its heave and pitch motions.

Figure 5.10 that the damper velocities reached are quite similar for both damping settings and are mostly concentrated in the $[-0.2 \text{ m/s} ; 0 \text{ m/s}]$ interval for both front and rear axles, for the low-speed test.

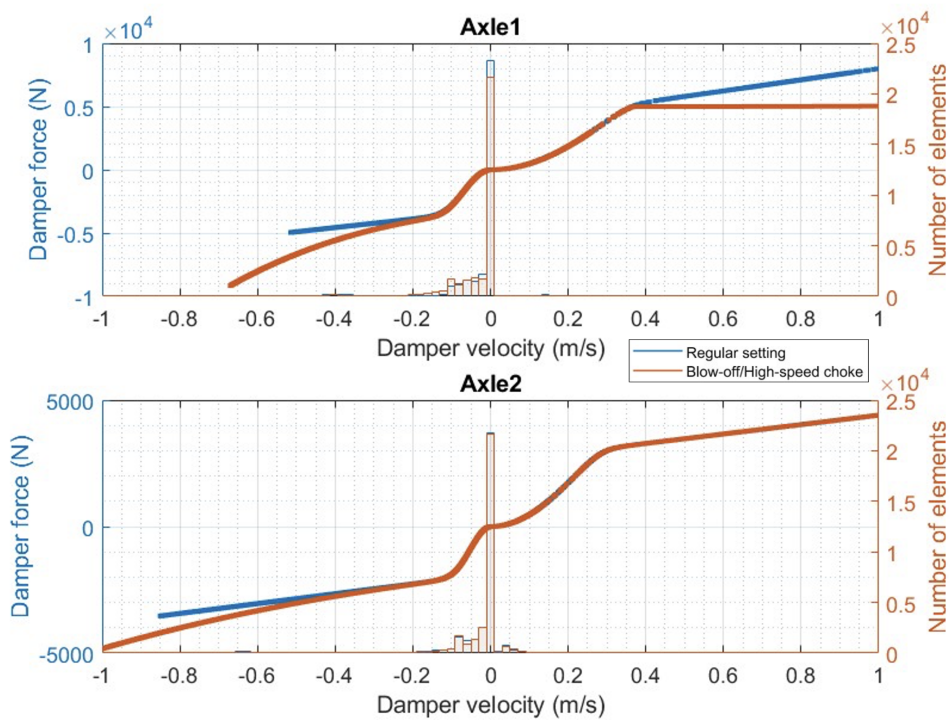


Figure 5.10: Damping curves - low-speed (30 km/h) jump test

According to 5.11, the damper velocities reached for the medium-speed test are quite similar for both damping settings and are mostly concentrated in

the $[-0.3 \text{ m/s}; 0 \text{ m/s}]$ interval for the front axle and in the $[-0.2 \text{ m/s}; 0 \text{ m/s}]$ interval for the rear axle.

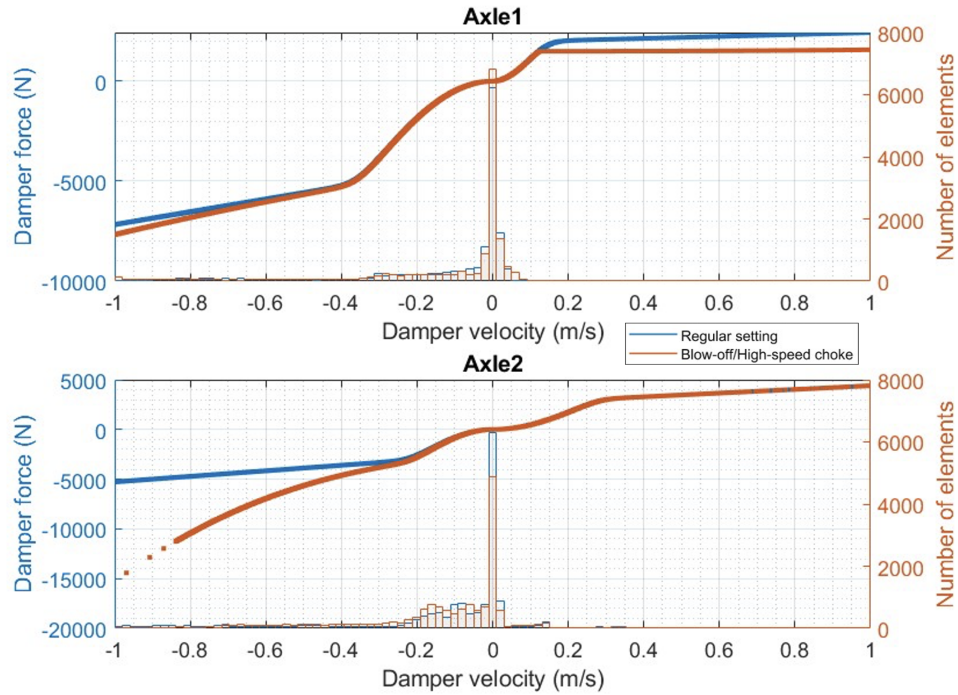


Figure 5.11: Damping curves - medium-speed (60 km/h) jump test

For the high-speed test, Figure 5.12 shows that the damper velocities reached differ according to the kind of damper used. For the front axle, the regular damper has velocities ranging from -0.2 m/s to 0 m/s mostly, while the damper with the blow-off and the high-speed choke valves have most velocities concentrated in the $[-0.9 \text{ m/s}; -0.2 \text{ m/s}]$ interval. For the rear axle, those intervals are $[-0.6 \text{ m/s}; -0.2 \text{ m/s}]$ and $[-0.4 \text{ m/s}; -0.2 \text{ m/s}]$ respectively.

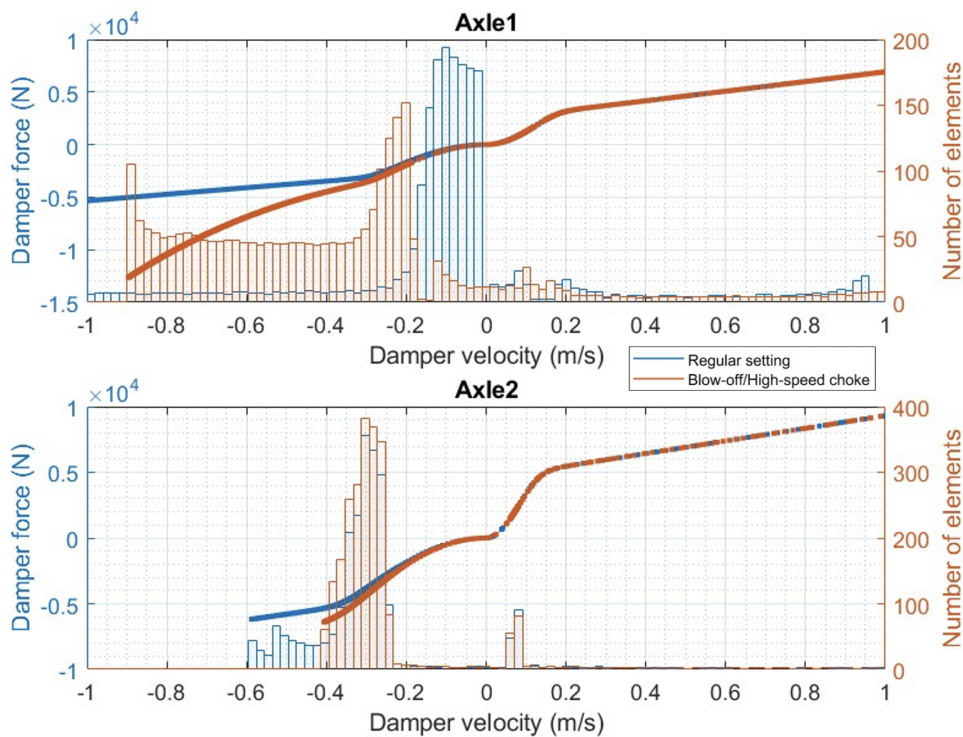


Figure 5.12: Damping curves - high-speed (90 km/h) jump test

For the low-speed test, it can be observed that the damping force almost reaches 17,500 N for the normal damper setting. It is achieved with a maximum value of around 2 g for the vertical acceleration of the chassis and 6 m/s for the damping velocity. The pitch varies in an envelope of 30° (with a maximum value of 20°) and the pitch rate peaks at $100^\circ/\text{s}$ when the truck bounces back after the landing.

With the blow-off and high-speed choke valves, the force has been reduced to approximately 7,500 N, which constitutes a decrease of almost 57%. However, this reduction is made possible by increasing the maximum vertical acceleration of the chassis to 5.2 g and the maximum damping velocity to 7.1 m/s, which is slightly above the critical value. The pitch envelope remained the same (30° between $+20^\circ$ and -10°) but the maximum pitch rate increased of almost $8^\circ/\text{s}$. Unlike the truck response to the bump, the response to the jump does not necessarily imply an important increase of the settling distance when the damper is equipped with a blow-off and a high-speed choke valve, as the settling distance increased from 25 m without the valves to 30 with.

Concerning the regular damper setting response for the medium-speed, it can be observed that the maximum damping force is once again quite high (more than 15,800 N). The maximum damping velocity is equal to the critical value (7 m/s) and the maximum vertical acceleration of the chassis is 4 g. The pitch is contained in an envelope that is slightly more than 20°. The maximum pitch rate is more than 80°/s.

The maximum damping force of the damper with the blow-off and the high-speed choke valves has been reduced to approximately 9,930 N, i.e. a decrease of 37%. However, this reduction is made possible by increasing the maximum vertical acceleration of the chassis to 9 g and the maximum damping velocity to 7.6 m/s, which is above the critical value. The pitch envelope has been reduced to 18°, as well as the maximum pitch rate which is equal to 68°/s. The system needs a bigger distance to settle, 50 m instead of 45 m.

Concerning the high-speed response, it can be observed that the damping force reaches a high value of 33,000 N for the regular damper setting. The maximum vertical acceleration of the chassis is around 6 g and the maximum damping velocity almost reaches 6 m/s. The pitch varies in an envelope of 15° and the pitch rate peaks at 90°/s when the truck lands. With this new configuration, the maximum vertical acceleration of the chassis is 5.6 g and the damping velocity reaches 7 m/s, which means 25,860 N is the lowest value of the maximum damping force it is possible to achieve without increasing the damping velocity above the critical velocity. The pitch envelope has been reduced to just 10° and the maximum pitch rate is reduced to 80°/s. The settling distance remains almost the same, increasing from 65 m to 70 m.

5.4 Acceleration and braking

After the optimisation process, the optimal damper settings for the acceleration and braking tests were determined and displayed in Table 5.3.

The damper curves are displayed in Figure 5.13.

Table 5.3: Optimised parameters - acceleration and braking test

| Front Axle | | |
|-------------------------|-------------|---------|
| | Compression | Rebound |
| Bleed valve coefficient | 100,000 | 100,000 |
| Rear Axle | | |
| | Compression | Rebound |
| Bleed valve coefficient | 700,000 | 700,000 |

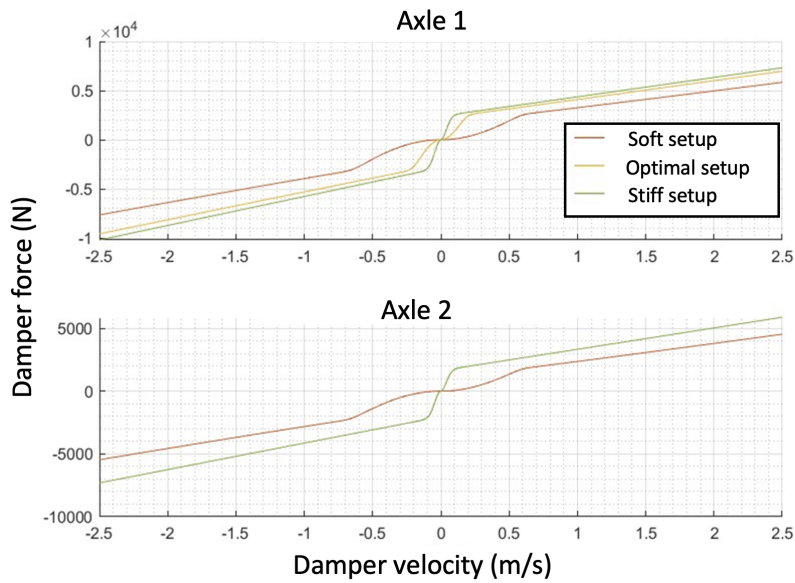


Figure 5.13: Damping curves - acceleration and braking test

Plotting the pitch as a function of time (Figure 5.14) is an indicator of the general behaviour of the car. As before, the same test is conducted with a soft and stiff setup to offer a benchmark. It can be observed that a soft setup entails a lot of oscillations in comparison to the optimal and the stiff setups. The stiff setup has a much slower response than the other two.

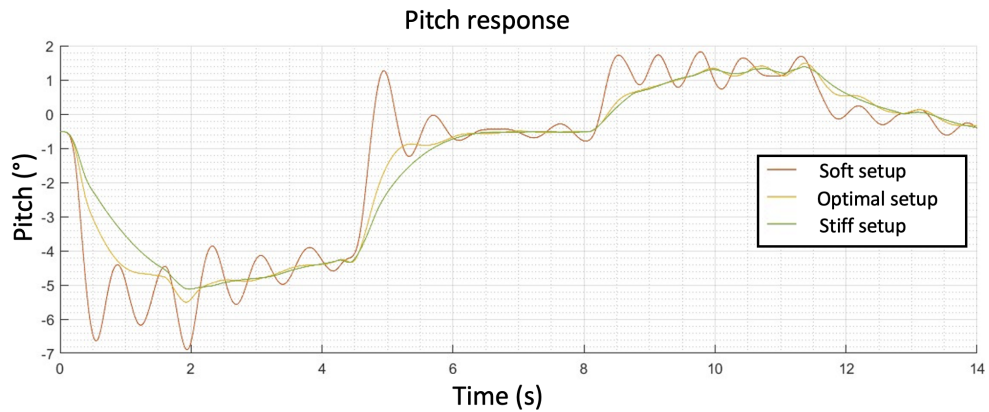


Figure 5.14: Pitch - acceleration and braking test

From the diagram of the pitch rate (Figure 5.15), it can be seen how more damping results in lower pitch rates. The optimal setup gives a good compromise between having low oscillations amplitudes and a fast enough response. This can be observed especially around the 5 seconds mark where it can be observed that the optimal setup is the one that settles the quickest.

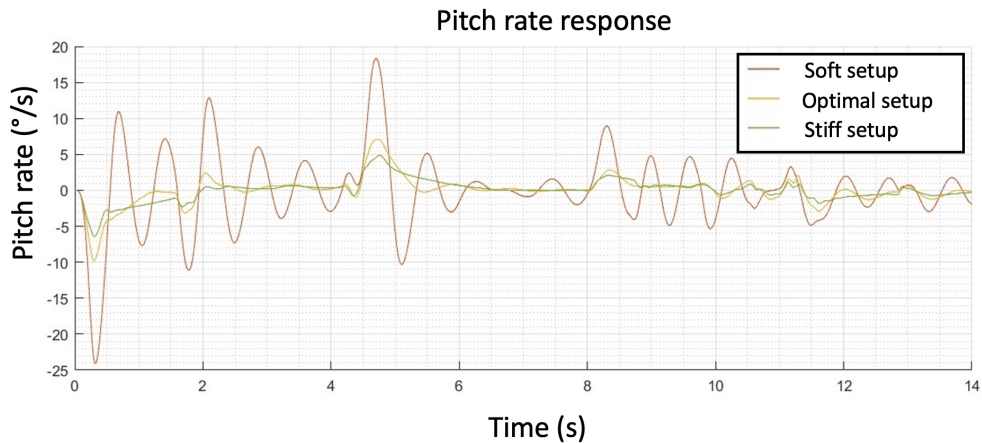


Figure 5.15: Pitch rate - acceleration and braking test

5.5 Steering

After the optimisation process, the optimal damper settings for the acceleration and braking tests were determined and displayed in Table 5.4.

Table 5.4: Optimised parameters - steering tests

| Front Axle | | |
|-------------------------|-------------|---------|
| | Compression | Rebound |
| Bleed valve coefficient | 150,000 | 150,000 |
| Rear Axle | | |
| | Compression | Rebound |
| Bleed valve coefficient | 150,000 | 150,000 |

The optimal setup was chosen in order to find a balance between control of the chassis motion and quickness of the response of the vehicle. The responses that were analysed to determine the optimal parameters were: roll angle, roll rate and load transfer ratio. The definition of this last one is a value between 0 and 1 where 0 indicates that all of the load transfer is happening on the rear axle while 1 means that all of the load transfer is happening on the front axle. This can be used during transients to see if the vehicle is trending more towards over or under-steering depending on if the current load transfer ratio is higher or lower than the static one (which for this vehicle is 0.45). This analysis tool proved particularly useful during the step steer analysis.

5.5.1 Step steer

From the roll (Figures 5.16) and roll rate responses (Figure 5.17), it is clear that the soft setup has higher oscillations. While the response for the stiffer curve seems optimal in this sense, the response of the chassis is also a lot slower. This becomes even more evident when looking at the load transfer ratio graph (Figure 5.18).

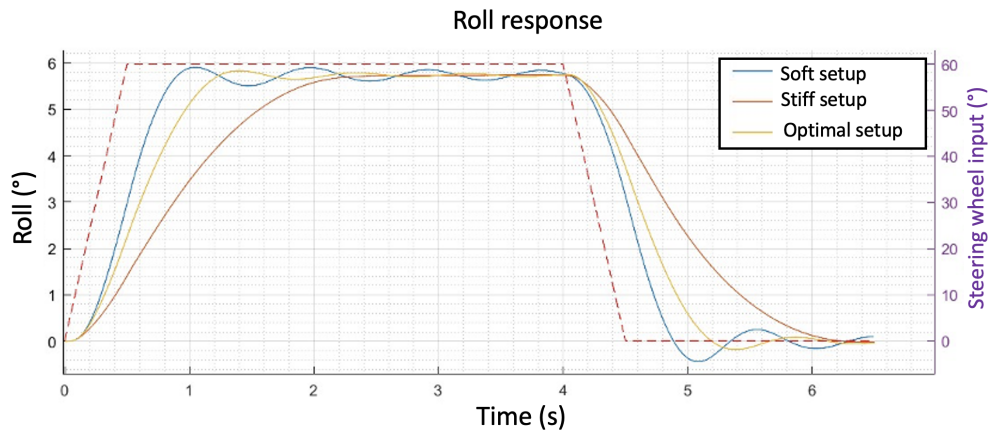


Figure 5.16: Roll - step steer test

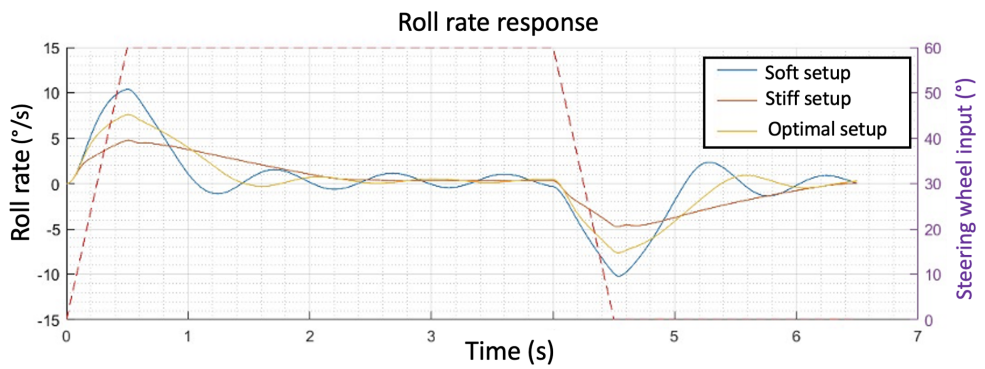


Figure 5.17: Roll rate - step steer test

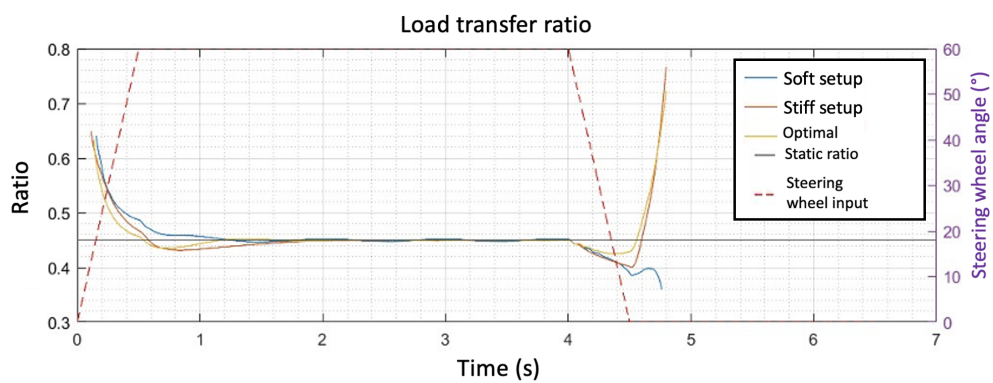


Figure 5.18: Load transfer ratio - step steer test

5.5.2 Double lane change

The situation is a lot less clear in a double lane change since the car never reaches steady state steering behaviour. This means that the vehicle is operating only in transient phases. While looking at the load transfer ratio (Figure 5.21), the stiff setup curve seems to be more constant, even if its value is a bit more on the over-steering side when compared to steady state operation. That said, the chassis takes a lot more time to react to the changes. This can be noticed in Figures 5.19 and 5.20, with the stiff setup curve has a delayed response when compared to optimal setup.

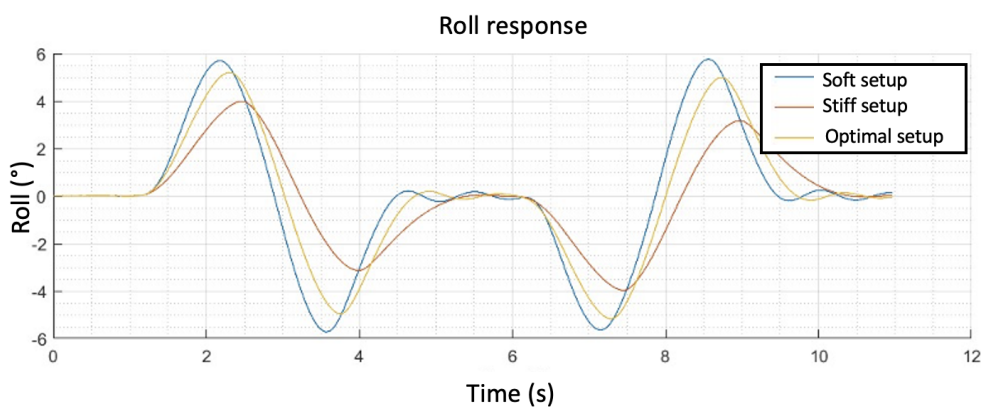


Figure 5.19: Roll - double lane change test

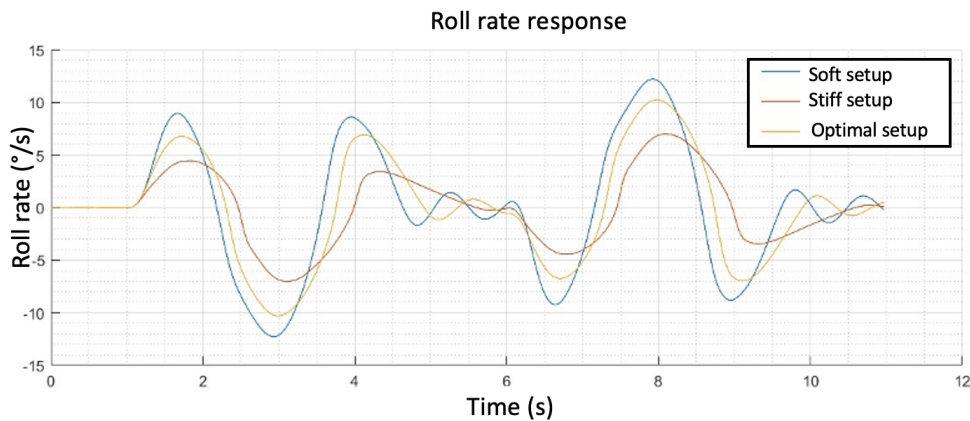


Figure 5.20: Roll rate - double lane change test

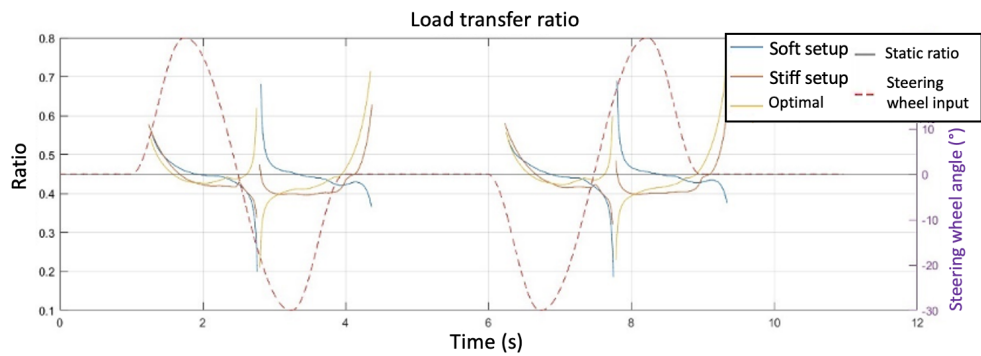


Figure 5.21: Load transfer ratio - double lane change test

5.6 Acceleration and braking test comparison

Table 5.5 shows the bleed coefficients of the three damper settings used.

Table 5.5: Bleed coefficients for comparison tests

| | Front | | Rear | |
|-------------------|-------------|---------|-------------|---------|
| | Compression | Rebound | Compression | Rebound |
| Chassis Stability | 32,000 | 85,000 | 13,500 | 13,500 |
| Jump (60 km/h) | 150,000 | 50,000 | 50,000 | 90,000 |
| Acceleration | 100,000 | 100,000 | 700,000 | 700,000 |

The pitch angle response is shown in Figure 5.22.

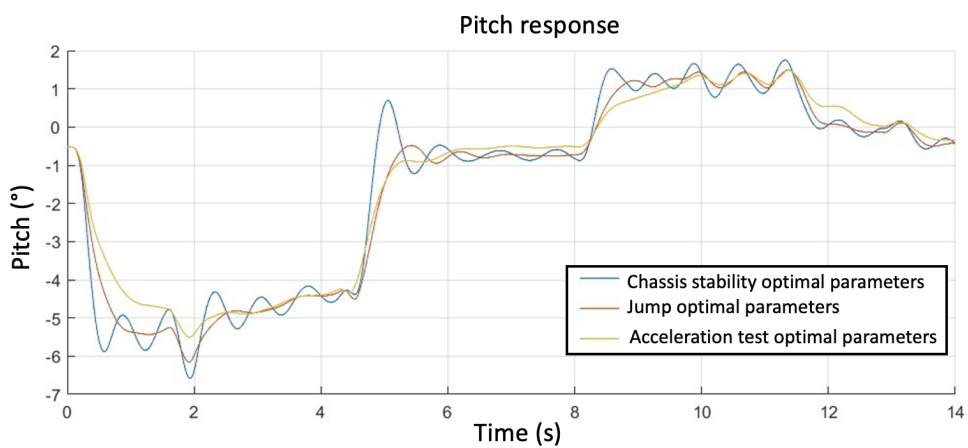


Figure 5.22: Pitch comparison - acceleration and braking

It is clearly visible that the parameters coming from the chassis stability optimisation result in higher oscillations. The setup optimised for the jump instead has a much better response, even if it still presents some oscillations around the 6 and 11 second marks. This can also be noticed in the pitch rate response graph displayed below (Figure 5.23).

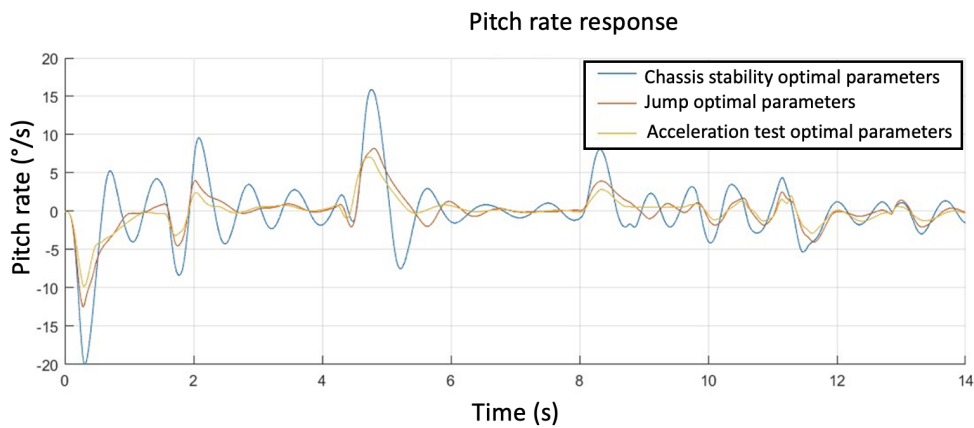


Figure 5.23: Pitch rate comparison - acceleration and braking

5.7 Steering test comparison

From the roll rate graph (Figure 5.24), it is clear that the chassis stability setup results in greater oscillations in comparison to the other two. This can be seen especially around the 5 and 10 second marks. The graphs for roll angle and load transfer ratio are shown in Figures 5.25 and 5.26 respectively. The jump setup is very close to the optimal setup in terms of response. It can be observed that these three setups are very similar in their response and that even the dampers optimised for the chassis stability and the jump tests have good steering responses.

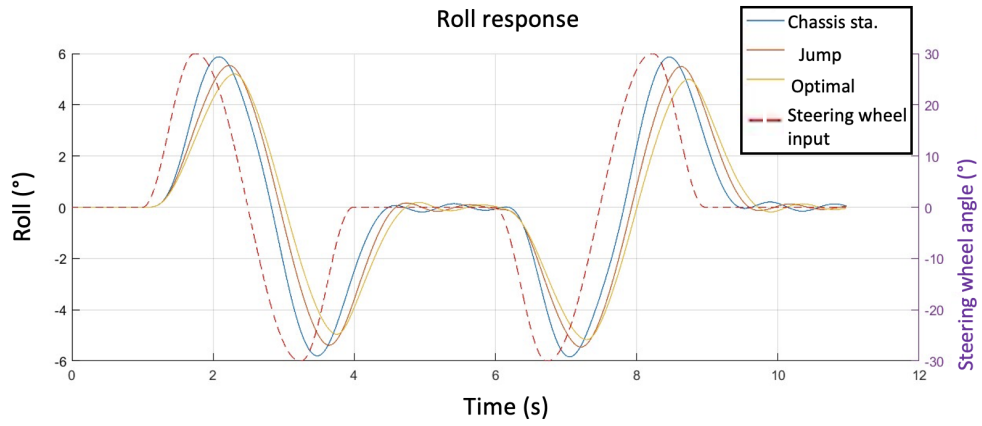


Figure 5.24: Roll comparison - double lane change

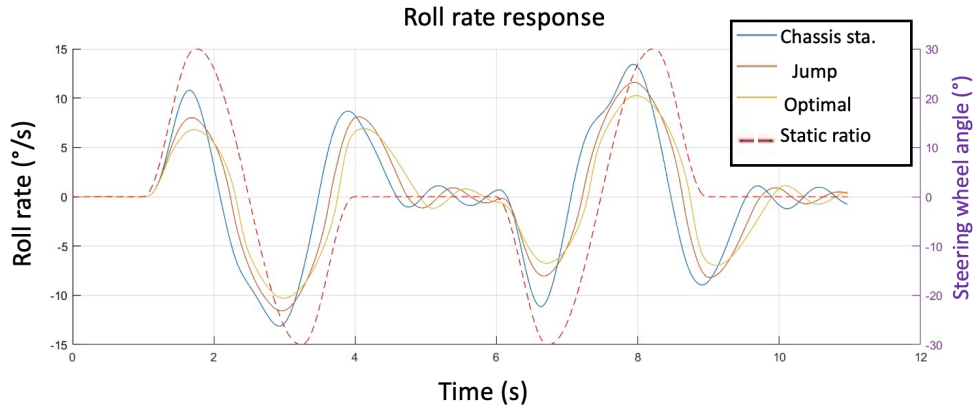


Figure 5.25: Roll rate comparison - double lane change

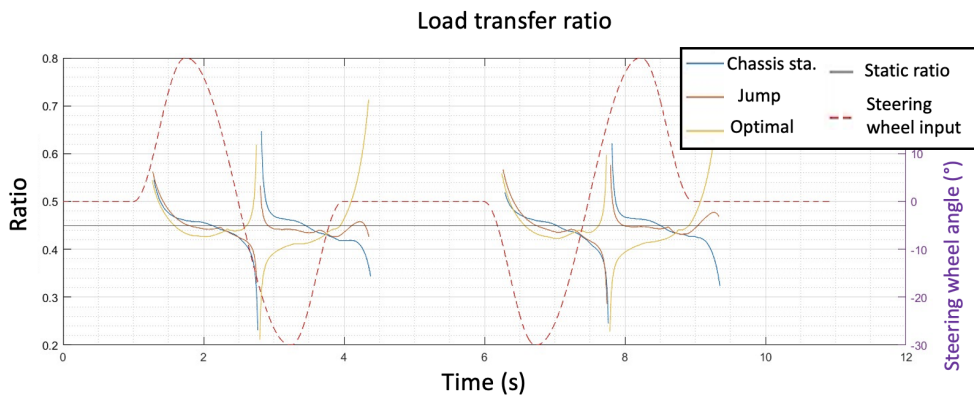


Figure 5.26: Load transfer ratio comparison - double lane change

5.8 Influence of friction

The results of this comparison are displayed in Table E.1. Concerning the bump absorption test, it can be observed that the results are almost the exact same with or without friction, even though they slightly differ when it comes to the pitch response, with both the maximum pitch rate and the pitch envelope being higher for the regular damper with internal friction, which is logical considering the fact that friction force is added. For the jump test, the results are almost exactly the same with or without internal friction in the damper with blow-off and high-speed-choke.

5.9 Influence of soft soil

The vertical dynamics of the chassis are shown in Figure 5.27. It can be observed that the vertical coordinate of the center of mass is generally lower for the soft soil, in comparison to the rigid soil. The pitch-roll envelope (Figure 5.28) shows that the chassis movement are also reduced significantly in the pitching direction.

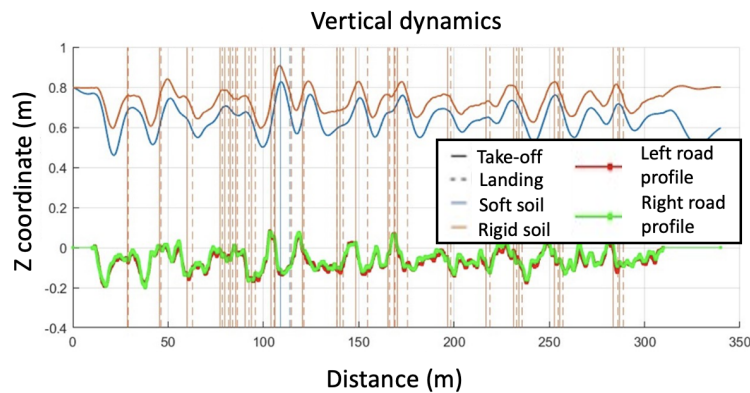


Figure 5.27: Vertical dynamics - soft soil influence

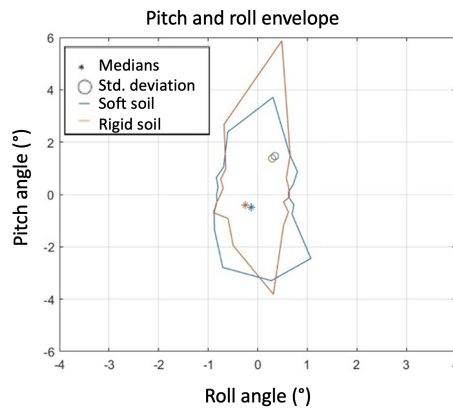


Figure 5.28: Pitch-roll envelope - soft soil influence

The most interesting results comes from the reading of the numerical values (Table 5.6). All of those are significantly reduced between the soft and the rigid soil. The airtime is the quantity where this reduction is the most prominent.

Table 5.6: Numerical results - soft soil influence

| | Soft soil | Rigid soil |
|----------------------------------|------------------|-------------------|
| Maximum damping force (N) | 5,521 | 8,397 |
| Maximum damping velocity (m/s) | 1.8 | 4.2 |
| Maximum damping displacement (m) | 0.15 | 0.17 |
| Airtime (%) | 1.3 | 25.8 |
| Load variation (N) | 1,322 | 2,614 |

Chapter 6

Discussions

6.1 Chassis stability

Optimising a suspension setup for the chassis stability test essentially means that the sprung and unsprung masses should move as independently as possible. Therefore the movement of the body is meant to be isolated from the one of the axles. To achieve this, the optimal setup for both scenarios had to be quite soft when compared to the other ones. One thing that brings together both the rock crawling and the dune riding optimal setups is that both need a low damping in the rear axle. If this is not the case, when riding over sharp bumps, the rear "kicks up" and unsettles the vehicle, making it harder to keep a good attitude towards the next obstacles.

The airtime percentage proved to be a good performance indicator in the sense that it "correlates" pretty well with other parameters that need to be improved such as the angle rates of the chassis and, particularly, the tyre load variation. That said, using it as the sole unrestricted optimisation parameter might not prove to be the best idea. A setup with large damping values in compression for the front suspension, for example, might give lower airtime percentages but result in damper forces that are too high because of its poor impact absorption capabilities.

If one was to automate this optimisation process, this is certainly something to take into account, meaning that a cost function would need to be developed where multiple parameters are considered and weighted.

6.2 Bump Absorption

When looking at the results for the bump absorption test, it can be concluded that as the speed of the vehicle increases, various parameters such as maximum damping force, maximum vertical acceleration of the chassis and settling distance tend to increase.

The utility of the damper with blow-off and high-speed-choke is proved: the regular damper setting generally provides higher maximum damping force across all speeds. Moreover, the blow-off/high-speed-choke damper setting offers advantages in terms of reduced maximum vertical acceleration of the chassis, especially at higher speeds. The regular setting tends to exhibit larger pitch values compared to the blow-off/high-speed choke setting, indicating more pronounced vehicle movements. The effectiveness of the damper with blow-off and high-speed-choke is due to the presence of the blow-off, which prevents the force from being too high, and the fact that the high-speed-choke compensates this low-compression damping. However, a longer stabilisation time after the bump is observed for the blow-off and high-speed-choke damper. This is due to the slower rebound entailing more damping.

It is important to notice that the maximum force happens at the bump impact, since low damping is used to keep the axle and the body "separated". This less damping force decreases acceleration.

Generally, a setting that is too soft will result in a high settling time after the bump and a risk of hitting the bump stops, while a setting that is too stiff will entail high forces, vertical acceleration and pitch rate.

Both damper settings exhibit relatively minor variations in temperature across different speeds, indicating consistent thermal behavior under different operating conditions.

6.3 Jump

Similarly to the bump absorption test, increasing vehicle speed generally results in higher maximum damping force, maximum vertical acceleration of the chassis and settling distance.

at a

The regular damper setting tends to provide higher maximum damping force compared to the blow-off/high-speed choke setting across different speeds. Contrary to all the previous optimisations, it was not possible to obtain a maximum damping force below 10,000 N with reasonable values of damping velocity and vertical chassis acceleration, for the damper with the blow-off and the high-speed choke valves. It is understandable since landing a 0.8 m high jump at 90 km/h requires a lot of damping force.

However, the blow-off/high-speed choke setting also leads to significantly higher maximum vertical acceleration of the chassis, suggesting a potential compromise in ride comfort. It is due to the fact that too much blow-off does not provide enough damping force, which increases acceleration. It even reaches more than 9 g for the medium-speed test (60 km/h). This is obviously not very pleasant comfort wise, but not dangerous, since this value only happens for a very short amount of time at impact, and is not sustained. For example, other drivers, such as F1 racers, can sustain more than 60 g at impact, such as Romain Grosjean did in a crash in 2021 with 67 g withstood.

The effectiveness of the damper with blow-off and high-speed-choke is due on the presence of the blow-off, which prevents the force for being too high, and the fact that the high-speed-choke prevents the bounce back effect after the jump landing. However, a longer stabilisation time after the bump is observed for the blow-off and high-speed-choke damper.

In that scenario, the maximum force happens at the landing, which means that a high damping is necessary to slow down the chassis during the landing phase. The heavier the impact, the harder to decrease the force even with the blow-off.

Similarly as for the bump absorption test, a setting that is too soft will result in a high settling time after the bump and a risk of hitting the bump stops, while a setting that is too stiff will entail high forces and pitch rate but also life-threatening values of vertical acceleration.

6.4 Acceleration and braking

When designing any dynamic system, the trade-off is usually between reducing the oscillatory behaviour and keeping the response quick. The chassis of a car is not so different, if the dampers are too soft the movement

will not be controlled, otherwise if it is too stiff the car will be too rigid.

During an acceleration run this is very evident as the force applied on the center of gravity induces pitch motion. Therefore, looking at the pitch and pitch rate during this kind of manoeuvre is almost like looking at a step response.

This means that the soft setup would be very uncomfortable to drive as a lot of oscillations would arise from simple acceleration manoeuvres. A setup that is too soft in this case will result in a lot of oscillations, especially during heavy deceleration. A setup that is too stiff on the other hand might slow down the dynamics of the chassis too much, as the chassis takes more time to reach its final steady state value. Increasing the damping force only on the rear axle is a good compromise that does not slow down the dynamics too much. The stiff setup instead results in a much slower movement of the chassis which might not be desirable in highly dynamic driving scenarios, since the vehicle has thus a delayed response.

6.5 Steering

What was said about the acceleration and braking responses can also be translated to the steering case, as in the damping should be enough to avoid any excessive oscillation but also not too much so that the chassis takes more time than necessary to settle down.

An added layer of complexity in the steering case is that there is an increased influence in the final results depending on how the damping is distributed between the front and rear axles. This was investigated through the load transfer ratio response and the objective was to keep it as constant as possible in a way that the vehicle would not change its behaviour too much throughout the cornering process. As the static load ratio between front and rear is about 0.45, keeping the same setup values between all dampers was found to be a good solution.

6.6 Acceleration and braking comparison

The chassis stability optimisation tends to cause more bouncing around throughout the simulation, suggesting it might struggle to keep the ride steady. It is due to the fact that this setting is too soft in comparison to the other two. Higher settling times are a result of too much undamped oscillations. The setup geared for jumps shows a much smoother response, with oscillations. The jump setting is stiffer and closer to the optimal setup for the double lane change. The response of these two settings is thus very similar. While prioritising stability is crucial for some setups like the chassis stability one, aiming for better jumps leads to setups that handle quick moves with more finesse. This analysis serves as a reminder of the intricate balance involved in adjusting vehicle setups to suit various driving scenarios. It underscores the importance of conducting comprehensive evaluations to ensure that these setups meet the required standards across all parameters.

6.7 Steering comparison

As observed in the results, the chassis stability has high oscillation amplitudes. It is due to the fact that this setting is too soft in comparison to the other two. This softness also entails a longer settling time. The jump setting is stiffer and closer to the optimal setup for the double lane change. The response of these two settings is thus very similar. The analysis highlights the effectiveness of the optimisation process in achieving satisfactory performance across different setups and driving scenarios. Despite some differences in roll rate behavior, all three setups demonstrate good steering responses, indicating the success of the optimisation process in balancing various performance metrics.

6.8 Influence of friction

For both tests, it has been seen in Section 5.8 that the internal friction of the damper has almost no influence on the performance of the vehicle on those cases. Not enough comparisons were made to be properly sure that it is the case for every scenario, but it can be suggested that the behaviour of the damper is not influenced by its internal friction, for both the regular damper and the one with blow-off and high-speed choke.

6.9 Influence of soft soil

Firstly, the fact that the vertical coordinate of the center of mass is generally lower is due to the sinkage of the car in the sand, which also implies that the airtime is almost null.

Concerning the fact that the values of numerical metrics (maximum damping force, velocity, displacement, airtime and load variation) are lower for the soft soil, this is due to the fact that a lot of the impacts are not absorbed just by the tyre-suspension assembly but also by the ground.

It is clear that the influence of the soft soil on the damper's behaviour and performance is non-negligible.

Chapter 7

Conclusions and future work

7.1 Conclusions

In conclusion, this thesis in collaboration with Öhlins Racing AB explored how to enhance the performance of off-road vehicle dampers, particularly in challenging terrains. Various configurations were examined and it was discovered that the settings of these dampers significantly impact the vehicle's performance. Different factors were assessed, such as the vehicle's stability, its ability to handle bumps and jumps, its acceleration and braking capabilities, and its steering response.

It was found that achieving an optimal damper setup is complex, and that it involves a delicate balance between stiffness and softness, and thus a fine tuning of many parameters, according to specific performance requirements.

Moreover, it was observed that the type of ground surface has a significant influence, as demonstrated by the influence of soft soil on damping characteristics. Soft terrain, such as sand, alters damper performance, resulting in different sensations compared to driving on harder surfaces.

Finally, it was concluded that internal damper friction has minimal impact on performance, validating the effectiveness of Öhlins Racing's technologies in minimising internal friction forces.

7.2 Future work

Although this thesis provides significant insights into off-road damper optimisation, there remain avenues for further research and improvement, particularly in refining the soft soil model and expanding its applicability in vehicle simulations, notably by modelling and testing more types of soft soil.

Concerning the damper model, different additional optimisation could be implemented, for instance position sensitive damping and acceleration sensitive damping.

The simulation strategy can also be improved. The dampers have only been tested for the Trophy truck, but it can be interesting to investigate damping performances for different type of off-road vehicle, such as motorbikes, quadbikes or buggies. Moreover, as explained previously in this thesis, off-roading implies a very wide field of scenarios, and an almost unlimited number of different tests and metrics could be run, investigated and analysed.

Future work in this area holds promise for advancing off-road vehicle dynamics and enhancing overall performance in challenging environments.

References

- [1] L. Drugge, “Springs and dampers,” in *Vehicle Components course*. Stockholm, Sweden: KTH, Vehicle Engineering Department, 2022.
- [2] Ansys, “Fundamentals of damping,” 2020. [Online]. Available: <https://courses.ansys.com/wp-content/uploads/2020/12/2.6.2-Fundamentals-of-Damping-New-Template.pdf>
- [3] N.-G. Nygren, “Inside TTX - The Öhlins TTX40 manual.” Öhlins Racing AB, 2005. [Online]. Available: https://ohlins.com/storage/043AE974273B07363A40C3EA29CB22D54ABA43D443A86E9467642502B66FB4C7/60c5304de56b463c973721dadbc29f54/pdf/media/3788ed7062df49f1a18911ad3343438c/OM_07430-01_Inside%20TTX40.pdf
- [4] G. Kokane, N. Ahamed, and R. Kharul, “A shock absorber design with position sensitive damper and its performance evaluation,” SAE Technical Paper, Tech. Rep., 2015.
- [5] “ISO 5167-1:2003 Measurement of fluid flow by means of pressure differential devices inserted in circular cross-section conduits running full - Part 1: General principles and requirements,” International Organization for Standardization (ISO), Tech. Rep., 1 March 2003.
- [6] A. Simms and D. Crolla, “The influence of damper properties on vehicle dynamic behaviour,” *SAE Transactions*, pp. 505–516, 2002.
- [7] E. Popova and V. L. Popov, “The research works of coulomb and amontons and generalized laws of friction,” *Friction*, vol. 3, pp. 183–190, 2015.
- [8] J. Wong, *Mechanics of Vehicle–Terrain Interaction*, 06 2022, pp. 77–219. ISBN 9781119719700

- [9] M. Fiolka, *1000 Miles to Glory: the history of the Baja 1000*. David Bull, 2004.
- [10] V. Pettit, “Introducing Stadium Super Trucks – SST What!?” The Checkered Flag, 2015. [Online]. Available: <https://www.thecheckeredflag.co.uk/2015/03/introducing-stadium-super-trucks-part-1-sst-what/>

Appendix A

Damping characteristics construction

A.1 Bilinear curve

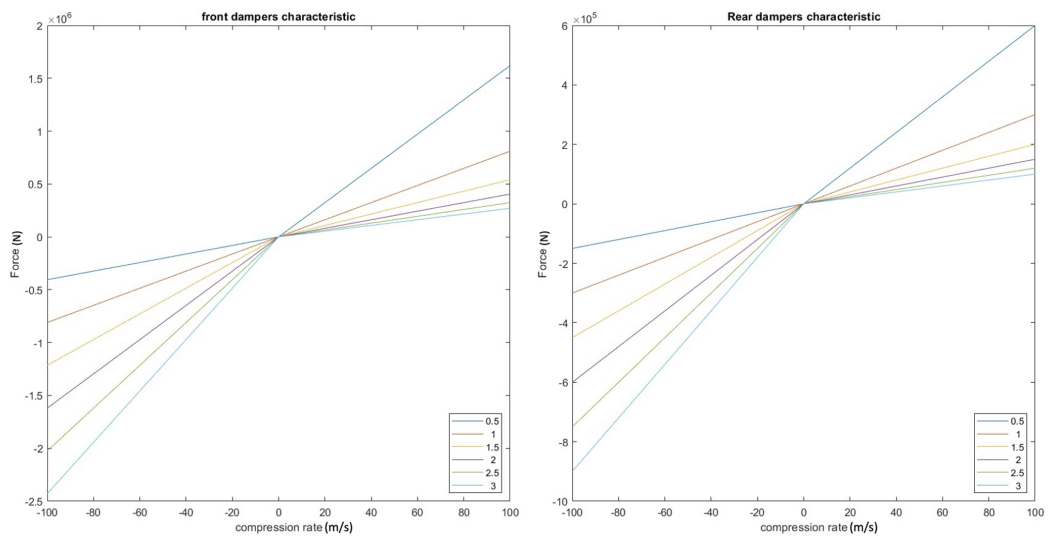


Figure A.1: Damper characteristics for different values of η - front and rear axle

A.2 Quadrilinear curve

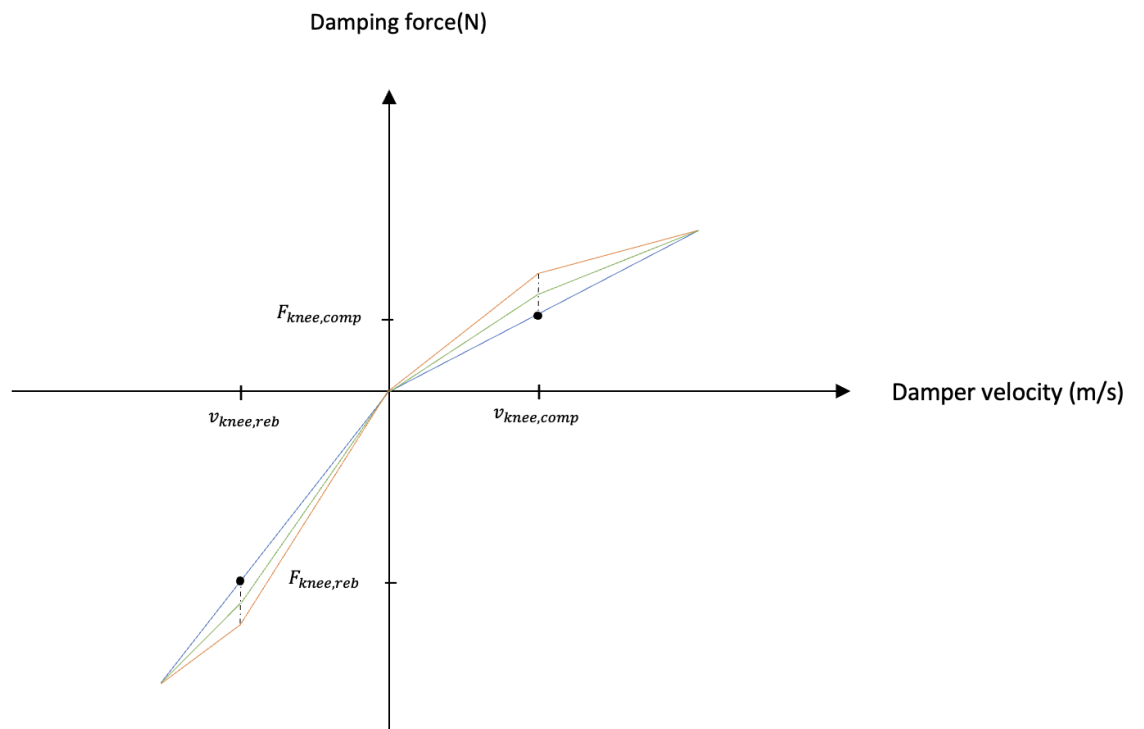


Figure A.2: Quadri-linear damper characteristic

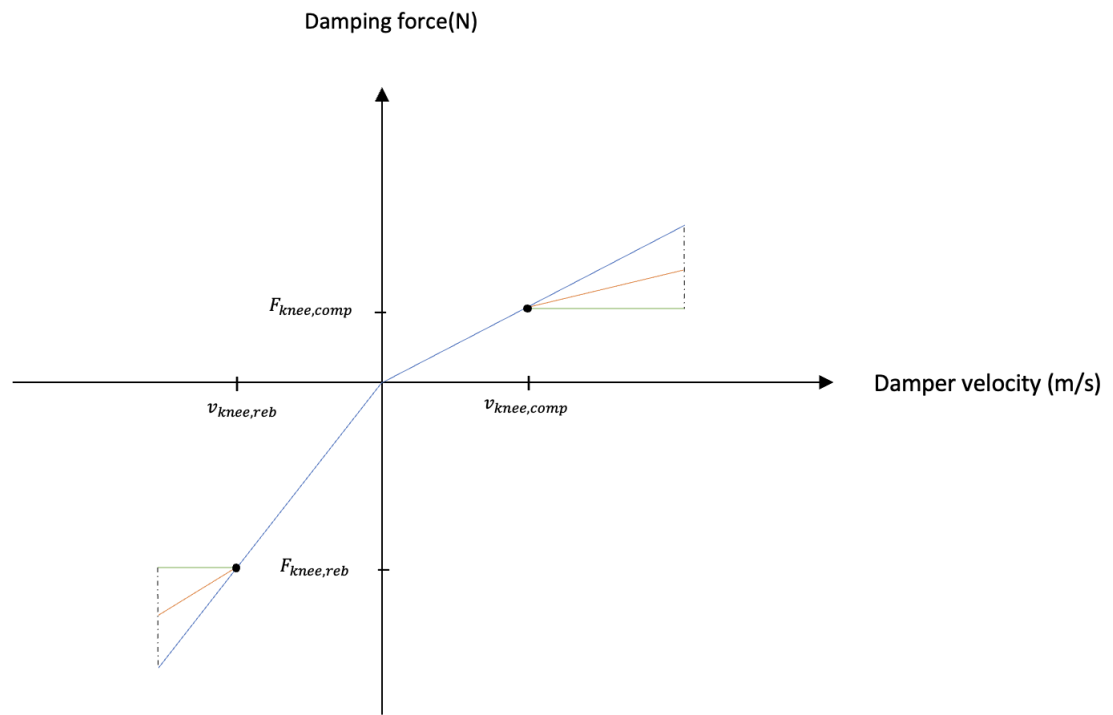


Figure A.3: Quadrilinear damper characteristic - different building method

A.3 Blow-off curve

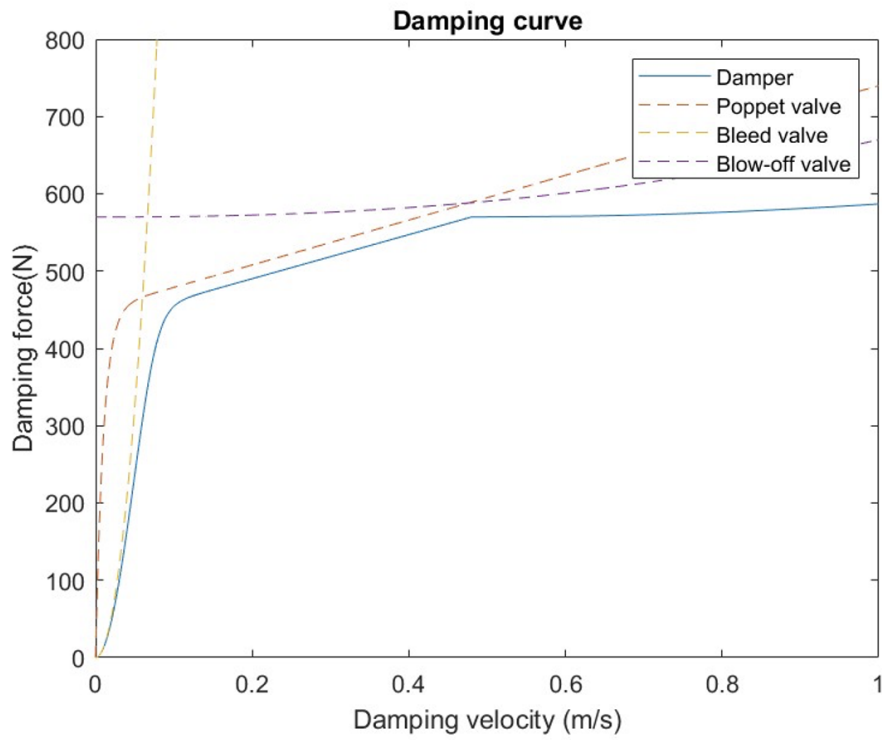


Figure A.4: Construction of a damping curve with blow-off - compression phase

A.4 High-speed choke curve

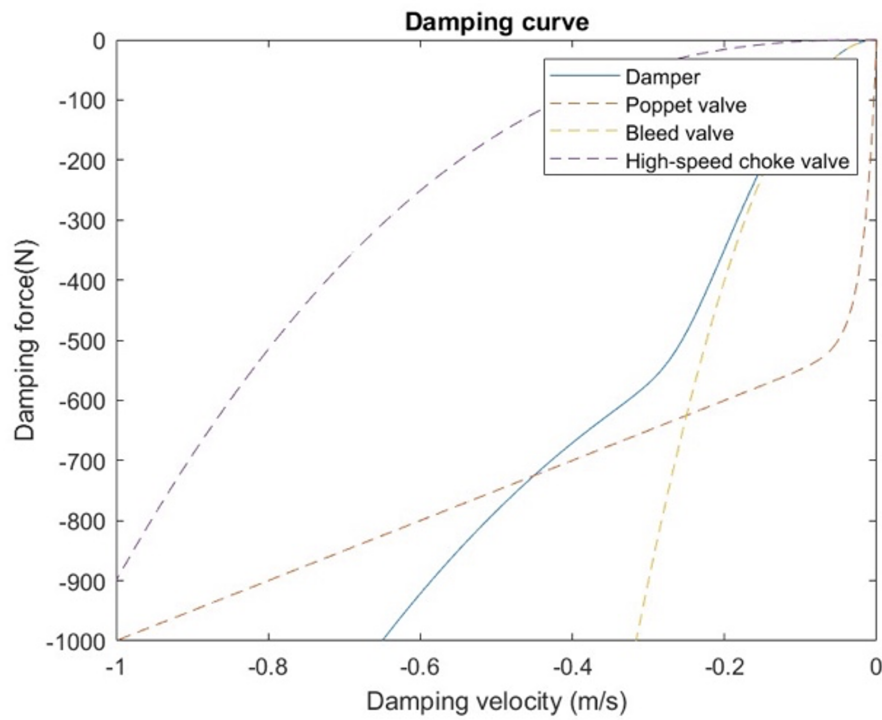


Figure A.5: Construction of a damping curve with high-speed choke - rebound phase

Appendix B

Chassis stability test results

B.1 Optimised parameters - chassis stability test

Table B.1: Optimised parameters - chassis stability

| | Low Speed (40 km/h) | | | | High Speed (80 km/h) | | | |
|-------------------------|---------------------|---------|-------------|---------|----------------------|---------|-------------|---------|
| | Front Axle | | Rear Axle | | Front | | Rear | |
| | Compression | Rebound | Compression | Rebound | Compression | Rebound | Compression | Rebound |
| Bleed valve coefficient | 15,000 | 300,000 | 10,500 | 10,500 | 32,000 | 85,000 | 13,500 | 13,500 |
| Poppet valve offset | 2,500 | 3,500 | 1,750 | 1,750 | 3,700 | 3,300 | 1,925 | 1,925 |
| Poppet valve slope | 2,500 | 3,500 | 1,750 | 1,750 | 2,750 | 3,800 | 1,925 | 1,925 |

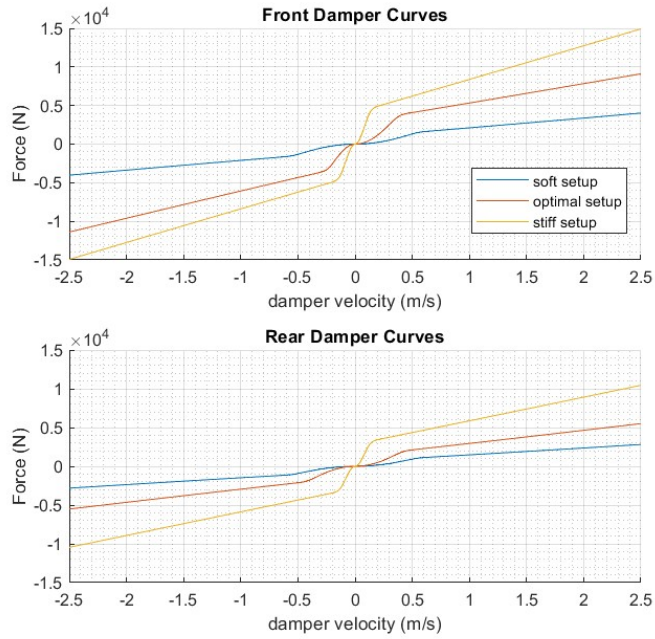


Figure B.1: Damping curves - high-speed (80 km/h) chassis stability test

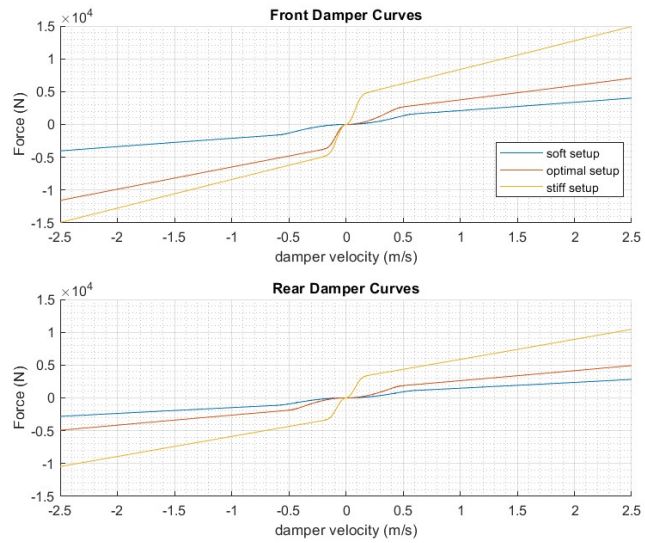


Figure B.2: Damping curves - low-speed (40 km/h) chassis stability test

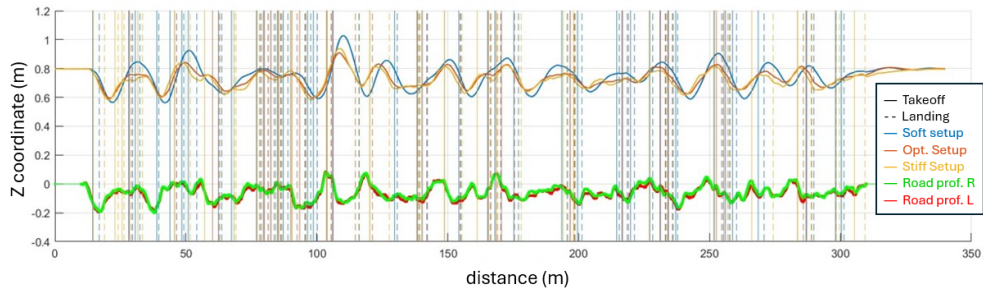


Figure B.3: Road profile - high-speed (80 km/h) chassis stability test

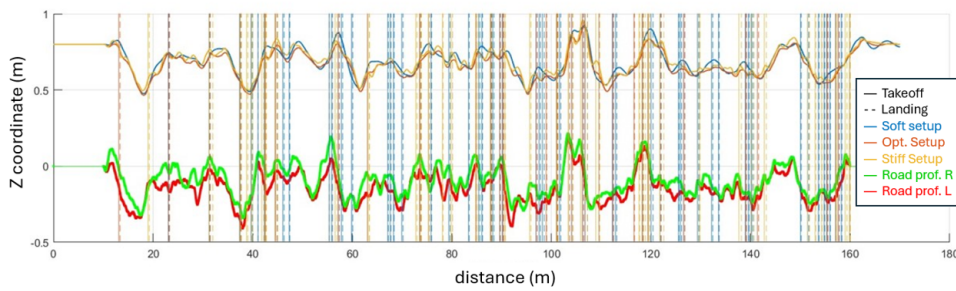


Figure B.4: Road profile - low-speed (40 km/h) chassis stability test

Appendix C

Bump absorption test results

C.1 Optimised parameters - bump absorption test

Table C.1: Optimised parameters - bump absorption test

| | Low-speed optimisation (30 km/h) | | | | Medium-speed optimisation (60 km/h) | | | | High-speed optimisation (90 km/h) | | | |
|------------------------------|----------------------------------|---------|-------------|---------|-------------------------------------|---------|-------------|---------|-----------------------------------|---------|-------------|---------|
| | Front axle | | Rear axle | | Front axle | | Rear axle | | Front axle | | Rear axle | |
| | Compression | Rebound | Compression | Rebound | Compression | Rebound | Compression | Rebound | Compression | Rebound | Compression | Rebound |
| Bleed valve coefficient | 50,000 | 150,000 | 50,000 | 50,000 | 200,000 | 150,000 | 200,000 | 150,000 | 200,000 | 400,000 | 200,000 | 400,000 |
| Poppet valve offset | 2,000 | 2,000 | 2,000 | 2,000 | 3,000 | 3,000 | 3,000 | 2,000 | 3,000 | 3,000 | 3,000 | 2,000 |
| Poppet valve slope | 2,000 | 2,000 | 2,000 | 2,000 | 2,000 | 1,000 | 1,000 | 1,000 | 3,000 | 3,000 | 3,000 | 3,000 |
| Blow-off valve coefficient | 100 | | 100 | | 1,000 | | 100 | | 100 | | 100 | |
| Blow-off valve offset | 1,000 | | 1,000 | | 4,000 | | 5,000 | | 5,000 | | 5,000 | |
| High-speed choke coefficient | | 500 | | 5,000 | | 100 | | 500 | | 1,000 | | 100 |

C.2 Numerical results - bump absorption test

Table C.2: Numerical results - bump absorption test

| | Low-speed optimisation (30 km/h) | | Medium-speed optimisation (60 km/h) | | High-speed optimisation (90 km/h) | |
|--|----------------------------------|---------------------------|-------------------------------------|---------------------------|-----------------------------------|---------------------------|
| | Regular setting | Blow-off/high-speed choke | Regular setting | Blow-off/high-speed choke | Regular setting | Blow-off/high-speed choke |
| Maximum damping force (N) | 11,352 | 4,633 | 13,263 | 9,625 | 20,011 | 9,092 |
| Maximum damping velocity (m/s) | 5.2 | 6.4 | 7.3 | 7.3 | 6.1 | 7.3 |
| Maximum vertical acceleration of the chassis (g) | 2.1 | 1.3 | 3.0 | 2.7 | 4.3 | 2.7 |
| Maximum pitch rate (°/s) | 41.7 | 38.0 | 28.0 | 34.5 | 32.5 | 29.5 |
| Pitch envelope (°) | 6.7 | 5.7 | 3.3 | 4.5 | 2.9 | 2.9 |
| Settling distance (m) | 65 | 75 | 85 | 120 | 120 | 150 |
| Temperature (°C) | 86.8 | 86.4 | 92.1 | 91.5 | 90.2 | 90.7 |

C.3 Low-speed bump absorption test (30 km/h)

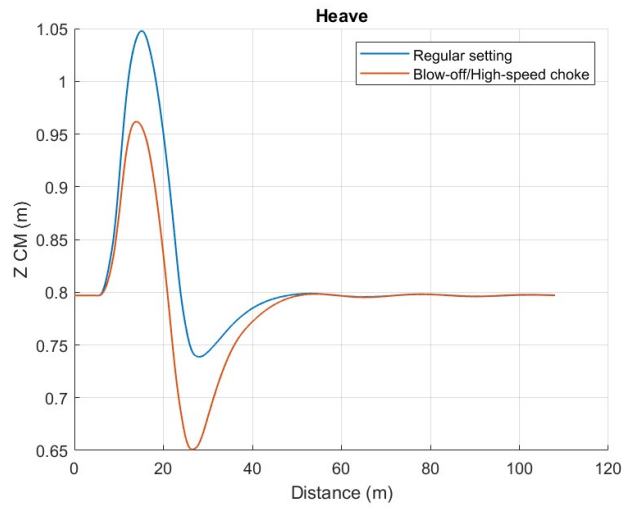


Figure C.1: Heave - low-speed (30 km/h) bump absorption test

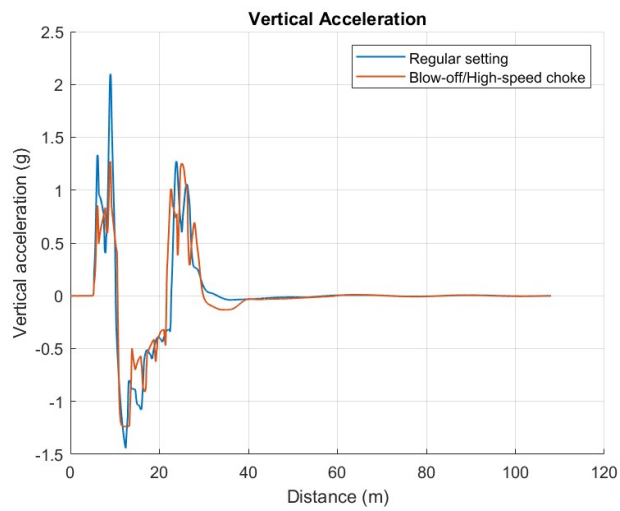


Figure C.2: Vertical acceleration - low-speed (30 km/h) bump absorption test

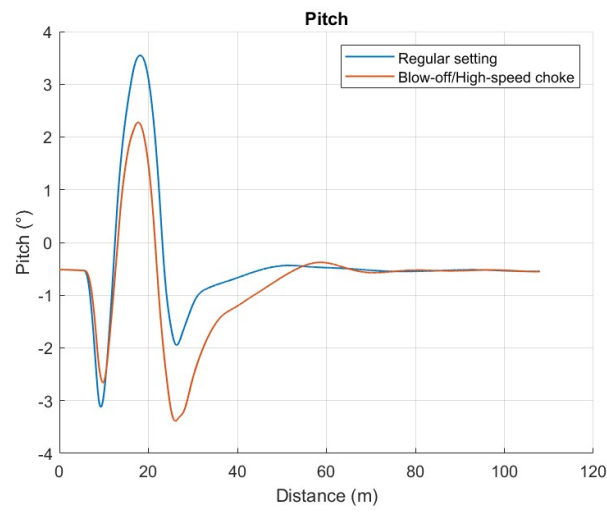


Figure C.3: Pitch - low-speed (30 km/h) bump absorption test

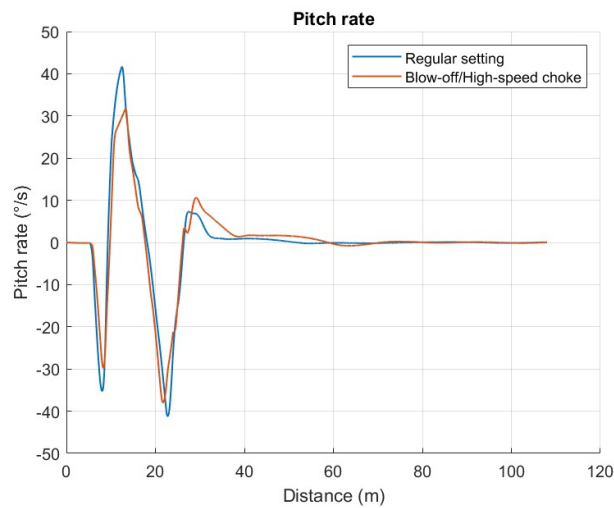


Figure C.4: Pitch rate - low-speed (30 km/h) bump absorption test

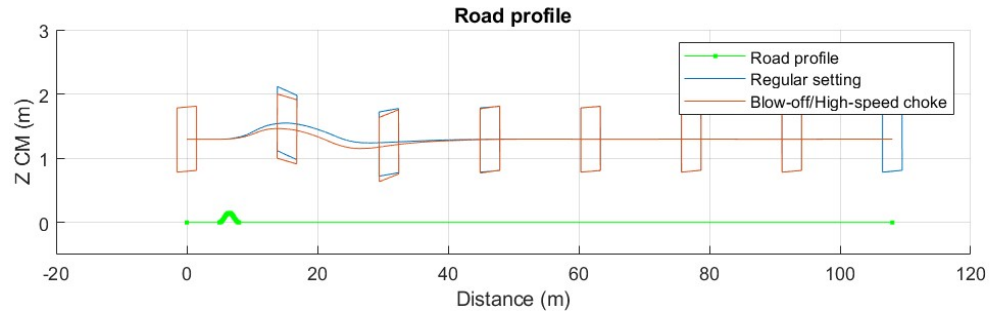


Figure C.5: Vehicle response - low-speed (30 km/h) bump absorption test

C.4 Medium-speed bump absorption test (60 km/h)

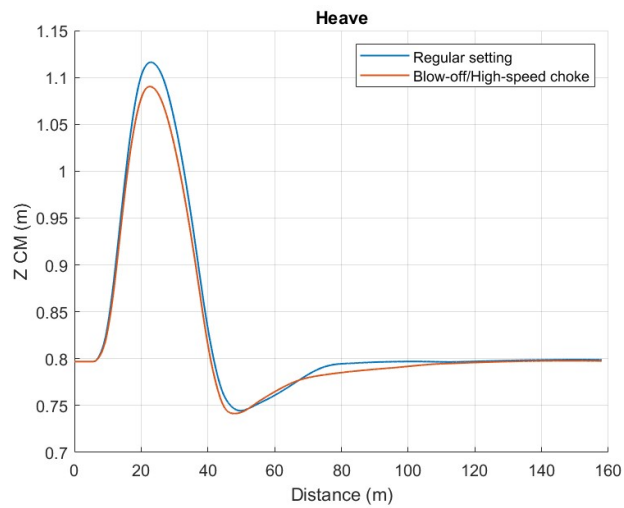


Figure C.6: Heave - medium-speed (60 km/h) bump absorption test

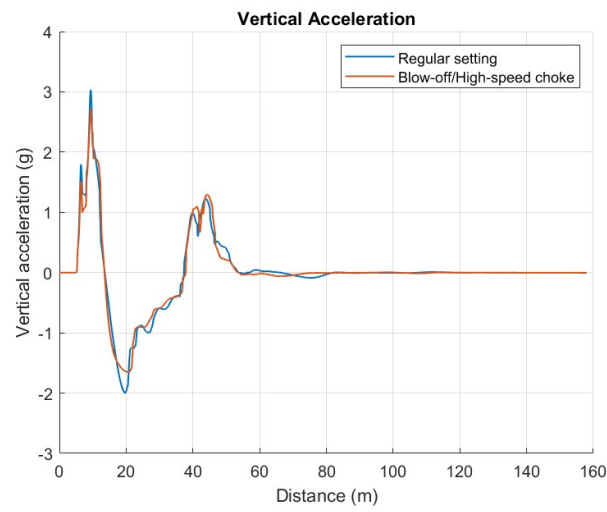


Figure C.7: Vertical acceleration - medium-speed (60 km/h) bump absorption test

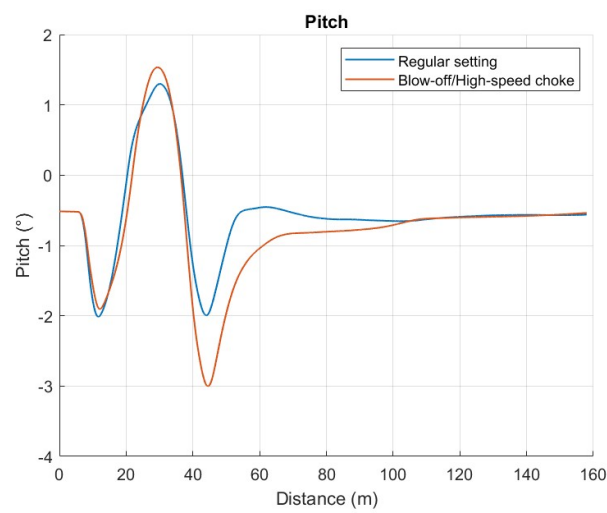


Figure C.8: Pitch - medium-speed (60 km/h) bump absorption test

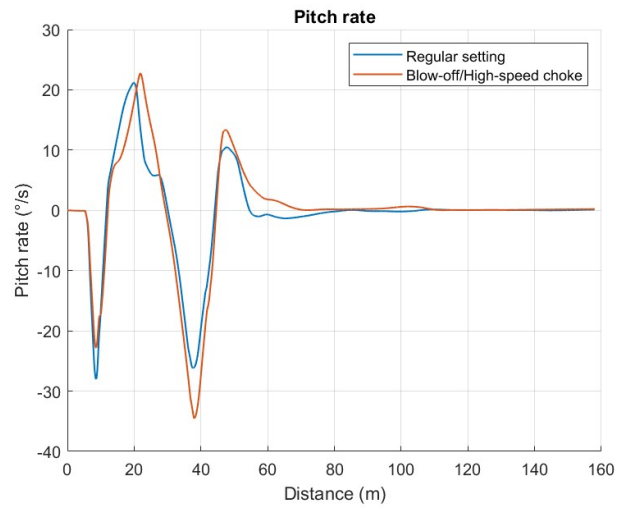


Figure C.9: Pitch rate - medium-speed (60 km/h) bump absorption test

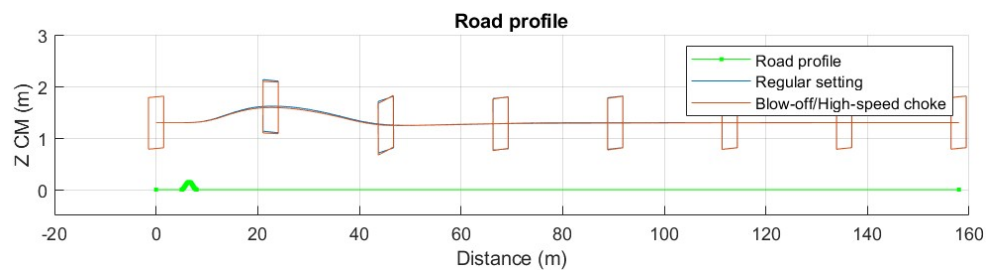


Figure C.10: Vehicle response - medium-speed (60 km/h) bump absorption test

C.5 High-speed bump absorption test (90 km/h)

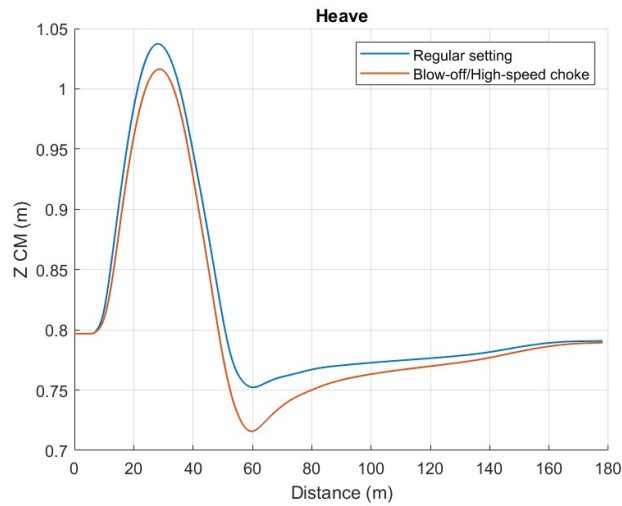


Figure C.11: Heave - high-speed (90 km/h) bump absorption test

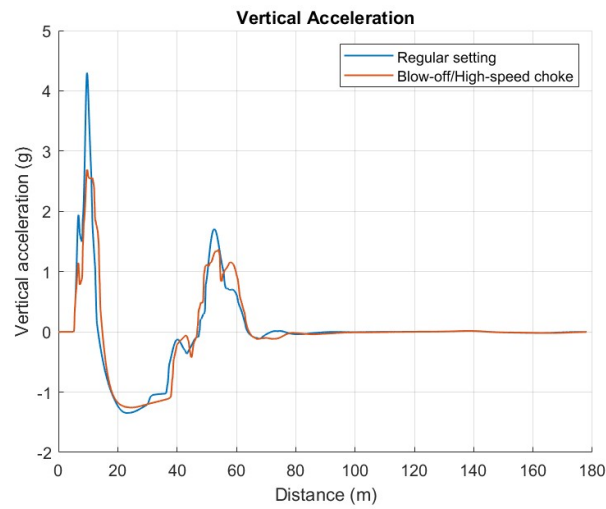


Figure C.12: Vertical acceleration - high-speed (90 km/h) bump absorption test

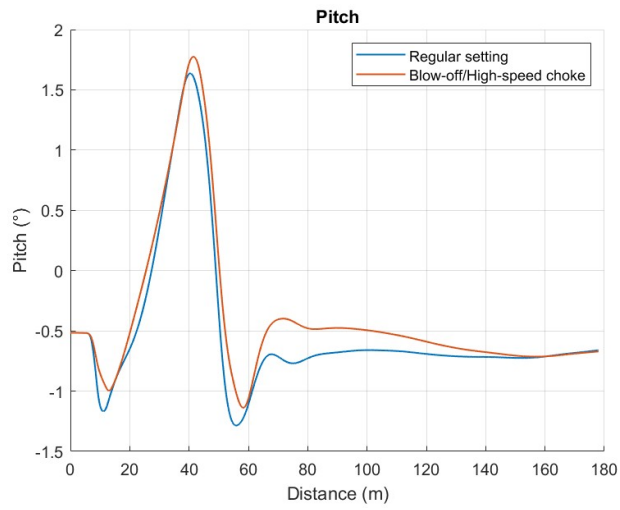


Figure C.13: Pitch - high-speed (90 km/h) bump absorption test

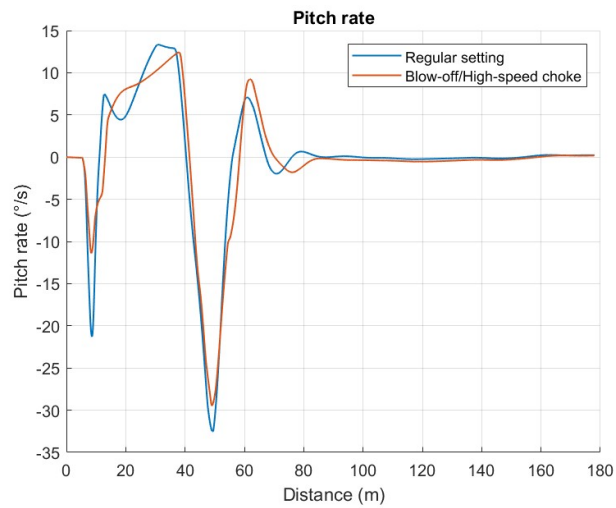


Figure C.14: Pitch rate - high-speed (90 km/h) bump absorption test

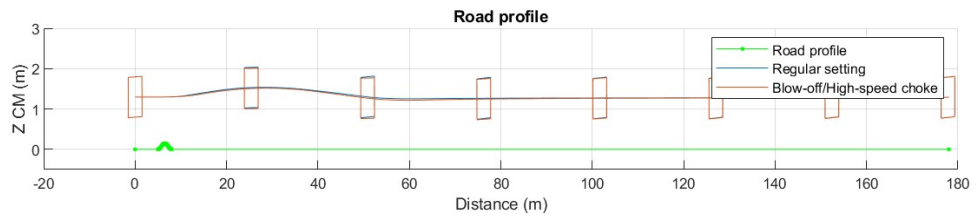


Figure C.15: Vehicle response - high-speed (90 km/h) bump absorption test

Appendix D

Jump test results

D.1 Optimised parameters - jump test

Table D.1: Optimised parameters - jump test

| | Low-speed optimisation (30 km/h) | | | | Medium-speed optimisation (60 km/h) | | | | High-speed optimisation (90 km/h) | | | |
|------------------------------|----------------------------------|---------|-------------|---------|-------------------------------------|---------|-------------|---------|-----------------------------------|---------|-------------|---------|
| | Front axle | | Rear axle | | Front axle | | Rear axle | | Front axle | | Rear axle | |
| | Compression | Rebound | Compression | Rebound | Compression | Rebound | Compression | Rebound | Compression | Rebound | Compression | Rebound |
| Bleed valve coefficient | 50,000 | 500,000 | 50,000 | 500,000 | 150,000 | 50,000 | 50,000 | 90,000 | 150,000 | 50,000 | 500,000 | 50,000 |
| Poppet valve offset | 5,000 | 3,500 | 3,000 | 2,000 | 2,000 | 5,000 | 3,000 | 3,000 | 3,000 | 3,000 | 5,000 | 5,000 |
| Poppet valve slope | 5,000 | 3,500 | 2,000 | 2,000 | 500 | 3,500 | 2,000 | 3,000 | 5,000 | 3,500 | 5,000 | 5,000 |
| Blow-off valve coefficient | 100 | | 100 | | 100 | | 100 | | 100 | | 100 | |
| Blow-off valve offset | 5,000 | | 4,400 | | 1,500 | | 8,000 | | 15,000 | | 25,000 | |
| High-speed choke coefficient | | 10,000 | | 1,000 | | 500 | | 10,000 | | 10,000 | | 10,000 |

D.2 Numerical results - jump test

Table D.2: Numerical results - jump test

| | Low-speed optimisation (30 km/h) | | Medium-speed optimisation (60 km/h) | | High-speed optimisation (90 km/h) | |
|--|----------------------------------|---------------------------|-------------------------------------|---------------------------|-----------------------------------|---------------------------|
| | Regular setting | Blow-off/high-speed choke | Regular setting | Blow-off/high-speed choke | Regular setting | Blow-off/high-speed choke |
| Maximum damping force (N) | 17,466 | 7,493 | 15,807 | 9,934 | 33,063 | 25,857 |
| Maximum damping velocity (m/s) | 5.7 | 7.1 | 7.1 | 7.6 | 5.9 | 6.9 |
| Maximum vertical acceleration of the chassis (g) | 2.2 | 5.2 | 4.2 | 9.1 | 6.2 | 5.6 |
| Maximum pitch rate (°/s) | 100.6 | 108.3 | 83.2 | 68.1 | 91.2 | 79.1 |
| Pitch envelope (°) | 29.7 | 31.0 | 20.2 | 17.6 | 14.6 | 11.3 |
| Settling distance (m) | 25 | 30 | 45 | 50 | 65 | 70 |
| Temperature (°C) | 87.6 | 87.2 | 90.9 | 91.3 | 97.0 | 96.6 |

D.3 Low-speed jump test (30 km/h)

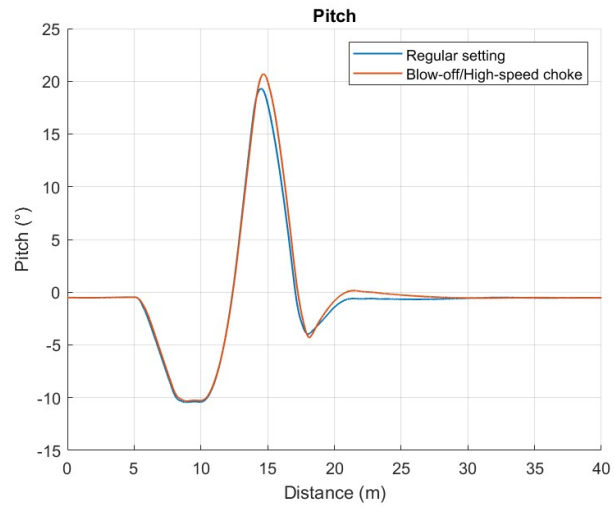


Figure D.1: Pitch - low-speed (30 km/h) jump test

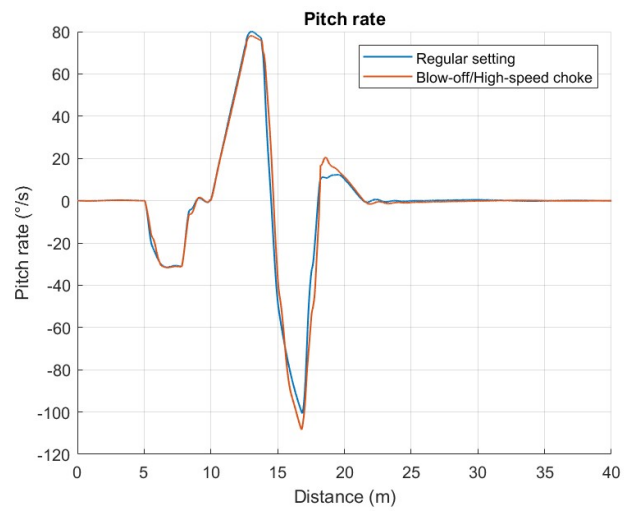


Figure D.2: Pitch rate - low-speed (30 km/h) jump test

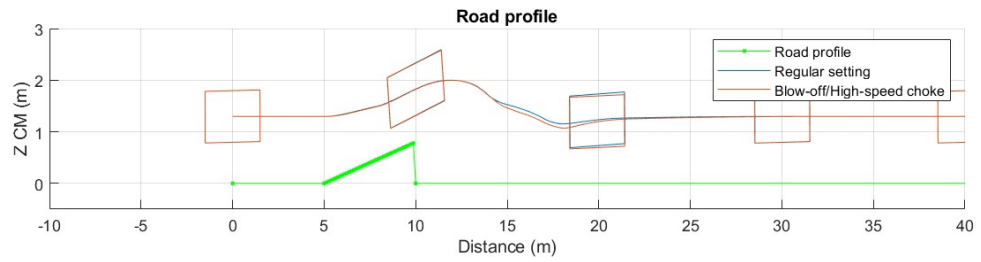


Figure D.3: Vehicle response - low-speed (30 km/h) jump test

D.4 Medium-speed jump test (60 km/h)

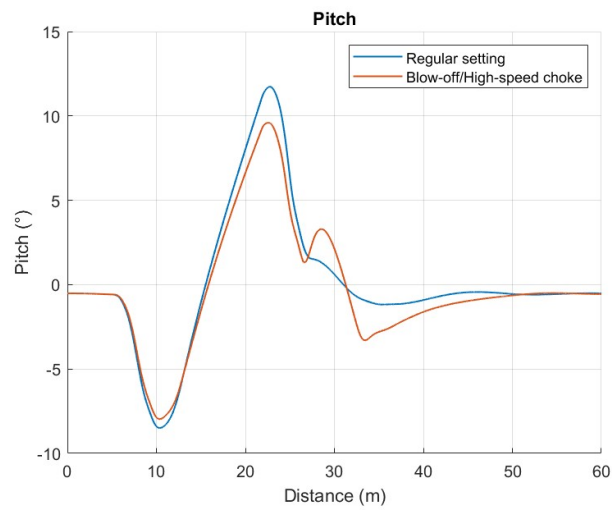


Figure D.4: Pitch - medium-speed (60 km/h) jump test

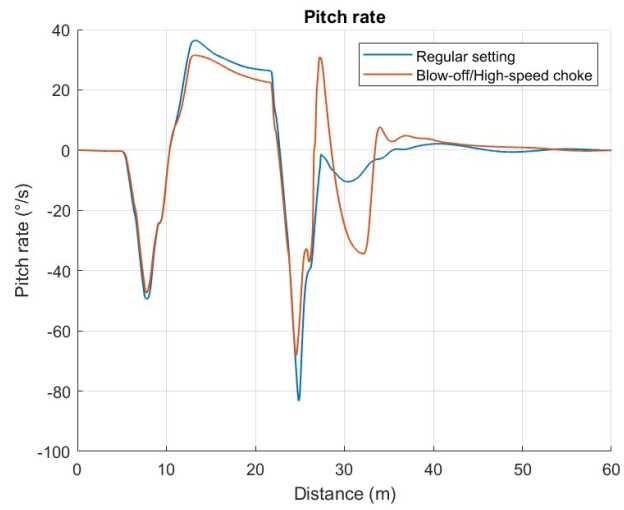


Figure D.5: Pitch rate - medium-speed (60 km/h) jump test

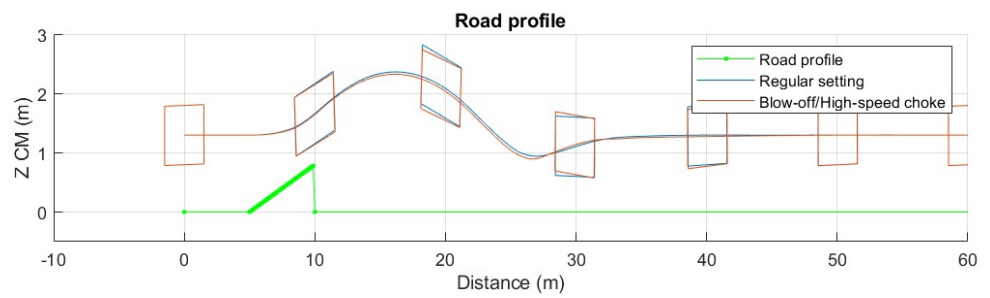


Figure D.6: Vehicle response - medium-speed (60 km/h) jump test

D.5 High-speed jump test (90 km/h)

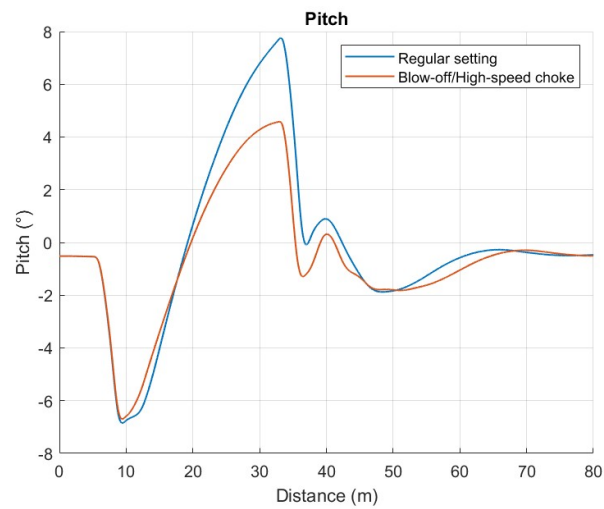


Figure D.7: Pitch - high-speed (90 km/h) jump test

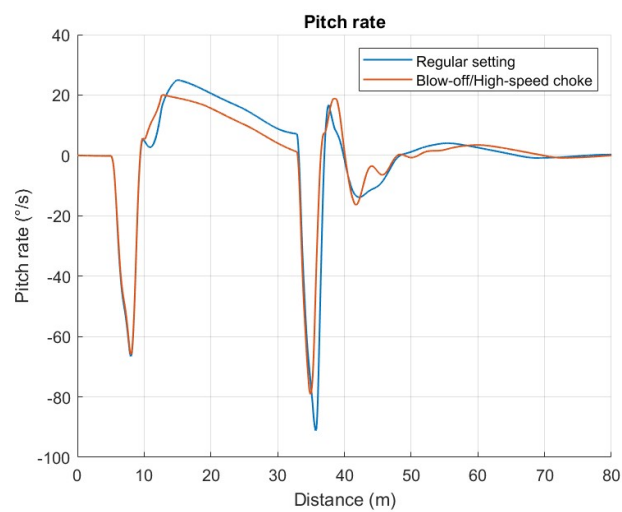


Figure D.8: Pitch rate - high-speed (90 km/h) jump test

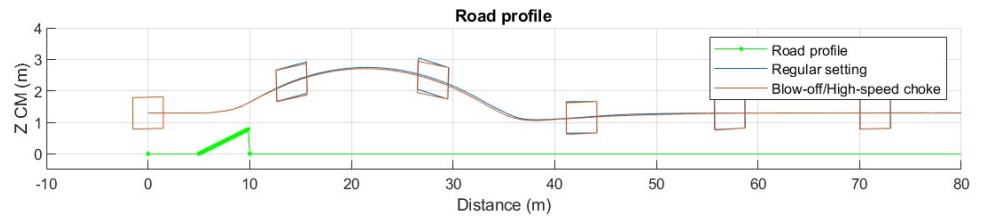


Figure D.9: Vehicle response - high-speed (90 km/h) jump test

Appendix E

Friction results

Table E.1: Numerical results - friction comparison

| | Medium-speed bump absorption test (60 km/h) | | Medium-speed jump test (60 km/h) | |
|--|---|---------------------------------------|---|--|
| | Regular damper without internal friction | Regular damper with internal friction | Damper with blow-off and high-speed-choke without internal friction | Damper with blow-off and high-speed-choke with internal friction |
| Maximum damping force (N) | 13,263 | 13,249 | 9,934 | 9,913 |
| Maximum damping velocity (m/s) | 7.5 | 7.5 | 7.6 | 7.6 |
| Maximum vertical acceleration of the chassis (g) | 3.0 | 3.0 | 9.2 | 9.0 |
| Maximum pitch rate (°/s) | 28.0 | 36.1 | 68.1 | 68.6 |
| Pitch envelope (°) | 3.3 | 5.1 | 17.6 | 17.7 |
| Settling distance (m) | 85 | 85 | 50 | 50 |
| Temperature (°C) | 92.1 | 91.7 | 91.3 | 91.3 |